

High-density, multi-functional neural probes for massively parallel read-out and control



FIG.1: MOLECULAR FOUNDRY BUILDING [1]



POLITECNICO
DI TORINO



5th of March – 31st of August 2018

VAHID DASTEJERDI Shervin, shervin.vahid@gmail.com

Supervisors: Stefano Cabrini, Nano-fabrication Facility Director, scabrini@lbl.gov & Vittorino Lanzio, PhD student, vittorinolanzio@lbl.gov

Thesis supervisors: Youla Morfouli & Liliana Prejbeanu

Place: Nano-fabrication Facility, Molecular Foundry, Lawrence Berkeley National Lab – 1 Cyclotron Road, Berkeley, 94720, California, United States of America

ACKNOWLEDGMENTS

First of all, I would like to thank Stefano Cabrini, who allowed me to work as a Research Affiliate during six months at the *Molecular Foundry* within the prestigious Lawrence Berkeley National Lab. He has always been helpful and gave me a lot of advices on the way to organize my work and to present my results.

Then, for accepting me as his assistant to work on the neural probes' project, I would like to thank Vittorino Lanzio. He taught me everything I had to know about the neural probes, from the biological point of view to the fabrication of the probes. He explained me the work he has been doing over the past two years to manage to develop optoelectronic neural probes. He has always been here to help when I was stuck in my research and he has always answered to all the questions I had the best way he could. I have learned a lot of things working besides him: how to be focused on your work, how to be patient and persistent to always keep moving on.

Also, I would like to thank Gianni Presti for helping me at my arrival to understand more deeply all the work that was going on about the neural probes: he introduced me to the topic and also to the way the *Molecular Foundry* is organized.

For training me on the different tools of the cleanroom, I would like to thank Mike Elowson, Arian Gashi, Aidar Kemelbay, Julia Szornel, Adam Schwartzberg, Stefano Dallorto and Scott Dhuey: they are always working hard to make sure users just have to focus on their projects without worrying too much about the tools' health.

For carrying out the electron-beam lithography for the development of the electrodes and of the optical elements of the project, I would like to thank Scott Dhuey: without his help, neural probes would not ever have been fabricated.

For nano-imprinting lenses on optical fibers used to test the gratings of the neural probes, I would like to thank Arian Gashi, Carlos Piña-Hernandez and Keiko Munechika.

Eventually, I would like to thank all the people I have met at the *Molecular Foundry*, users, technicians, students, who make this place a very special one where science always rhymes with happiness and mutual aid.

A special thank to Minji Hong, Monica Lorenzon and Fabrizio Riminucci for being part of the funny break times for these six months.

GLOSSARY

ALD: Atomic Layer Deposition, **cf. Appendix 1 for explanation**

APs: Action Potentials are electrical signals triggered by one neuron to carry the information towards another neuron. They involve ions flux in and out the neuron's membrane.

CCP: Capacitively-Coupled Plasma, **cf. Appendix 1 for explanation**

ICP: Inductively-Coupled Plasma, **cf. Appendix 1 for explanation**

ImageJ: Open-source software that can be used to carry out image analysis

L-edit®: Commercial software that can be used to design layout for micrometric devices

LPCVD: Low-Pressure Chemical Vapor Deposition, **cf. Appendix 1 for explanation**

PECVD: Plasma-Enhanced Chemical Vapor Deposition, **cf. Appendix 1 for explanation**

RF: Radio-Frequency

RIE: Reactive Ion Etching, **cf. Appendix 1 for explanation**

rpm: revolution-per-minute = number of revolution per minute the chuck on which the wafer is resting during the spin-coating of a photoresist is doing

SEM: Scanning Electron Microscope, **cf. Appendix 1 for explanation**

VHF: Very High Frequency

Outline

Acknowledgments	1
Glossary	1
Figures	3
Tables	4
I) Introduction	5
A) Purpose of the report	5
B) The Lawrence Berkeley National Laboratory (LBNL)	5
II) Biological background and interest of a three-function neural probe	6
A) The neurons' communication inside the brain	6
1) The neurons' structure	6
2) An electrical signal allows for the communication between several neurons	7
3) Translation of the action potential into a chemical signal at the junction between two neurons	8
B) Optogenetics: neural manipulation with light	9
C) Comparison between the different brain signals' recording techniques	10
D) What parameters must be taken into account when developing a neural probe?	13
E) State-of-the-art for the Michigan neural probes	14
III) The Michigan probes developed at the Molecular Foundry	16
A) Probes' structure and design	16
1) Electrical part	17
2) Optical part	17
B) Fabrication process	21
1) Alignment marks development	21
2) Process for the optical part: waveguides, ring resonators and gratings development	22
3) Process for the electrical part: electrodes, wires and pads development	22
4) Releasing the probes	23
5) Electrodes electroplating	26
C) Budget	27
IV) Results and discussion	27
A) Fabrication of optoelectronic probes	28
B) Tests of the optical components integrated on the probes	28
1) Fiber gluing	29
2) Test of the ring resonators	30
3) Test of the focusing gratings	31
4) Power measurements from the probes and sources of losses	32
C) Possible improvements and next steps for the project	36
1) How to obtain a better fiber-waveguide coupling efficiency?	36
2) Further modifications of the neural probes	36
3) In-vivo tests of the optoelectronic probes	36
V) Conclusion	37
Bibliography	38
Appendix 1: Tools used for the project	41
Exposition tools	41
Tool 1: UV Photolithography	41
Tool 2: Electron-Beam Lithography	41
Etching tools	41
Tool 1: Reactive Ion Etching (RIE)	41
Tool 2: Inductively-Coupled Plasma Reactive Ion Etching (ICP RIE)	42

Tool 3: Capacitively-Coupled Plasma (CCP RIE) or Viper	42
Deposition tools.....	43
Tool 1: Plasma-Enhanced Chemical Vapor Deposition (PECVD)	43
Tool 2: Evaporator	43
Tool 3: Atomic Layer Deposition (ALD).....	43
Characterization tools.....	43
Tool 1: Scanning Electron Microscope	43
Tool 2: Profilometre	43
Appendix 2: Power computation from the gratings	44
Appendix 3: Insertion of thin probes inside a mice's brain.....	44

FIGURES

<i>Fig.1:</i> Molecular Foundry building [1]	0
<i>Fig.2:</i> View of the Cyclotron in the foreground and of the San Francisco Bay Area in the background, from the LBNL [2].....	5
<i>Fig.3:</i> Representation of a neuron [4]	6
<i>Fig.5:</i> Structure of a neuron [7]	6
<i>Fig.4:</i> Internal organization of the brain with the different kinds of cells. There are several types of glial cells: oligodendrocyte, microglia, astrocytes, each having their own function [6].....	6
<i>Fig.6:</i> The action potential generation, temporal summation [8]	7
<i>Fig.7:</i> Timecourse of an action potential [8]	7
<i>Fig.8:</i> First step of the AP propagation [8].....	7
<i>Fig.9:</i> Second step of the AP propagation [8]	8
<i>Fig.10:</i> Third step of the AP propagation [8].....	8
<i>Fig.11:</i> Transmission of the electrical AP thanks to chemical neurotransmitters at the interface between the pre and the post-synaptic neurons [8]	8
<i>Fig.12:</i> When the channelrhodopsin is present in the algae (CW2), it goes away from light; when the channelrhodopsin is not present in the algae, it does not move when it is exposed to light [15]	9
<i>Fig.13:</i> Functioning of different opsins. (A) The two channel proteins are not illuminated: they are closed. (B) When illuminated with light with the right wavelength, the channels open and let ions flow inside the cell. (C) Activation of ChR2 allows for the triggering of APs whereas HR activation suppresses the APs [16]	9
<i>Fig.14:</i> Different opsins with specific activation wavelength can be used [18]	9
<i>Fig.15:</i> Insertion location of several recording techniques [27].....	10
<i>Fig.16:</i> Spatial and temporal resolutions of several recording techniques [28].....	11
<i>Fig.17:</i> EEG principle [34]	11
<i>Fig.18:</i> MEA structure: the electrodes are located at the center of the square [36].....	11
<i>Fig.19:</i> Microwires tip not insulated [37]	12
<i>Fig.20:</i> Picture of a multi-functional fiber [38]	12
<i>Fig.21:</i> Utah-type probe [23]	12
<i>Fig.22:</i> Michigan-type probe [23]	12
<i>Fig.23:</i> Sketch showing the spatial relationships between a neuron and a substrate-integrated electrode and the analogue passive electrical circuit [41]	13
<i>Fig.24:</i> High-density neural probe [50].....	14
<i>Fig.25:</i> Neural probe with micro-fluidic channels for drug delivery inside the brain [51].....	14
<i>Fig.27:</i> Measurements showing the effects of the drug delivery inside the brain: the action potentials due to the seizure are reduced with Baclofen [52].....	15
<i>Fig.26:</i> Double-functionality neural probe: electrodes and micro-fluidic channels [52].....	15
<i>Fig.29:</i> The gratings of the probe are radiating light [53].....	15
<i>Fig.28:</i> Optoelectronic probe combining electrodes and gratings to stimulate neurons and record the induced electrical signal [53]	15
<i>Fig.30:</i> Neural probes integrated with micro LEDs to shine light inside the cortex [56]	15
<i>Fig.31:</i> Picture showing the structure of the probe compared with a hair	16
<i>Fig.32:</i> Probe glued on the PCB using Epoxy glue, before the wire-bonding	16
<i>Fig.33:</i> Sketch of a probe inserted inside the cortex of the brain	16
<i>Fig.34:</i> Sketch of the 2-level shank developed up to now: the lower level is composed of optical components for optogenetics, the upper one is composed of electrodes to record the neural signals	17
<i>Fig.36:</i> SEM images of the pads of the bonding area	17

<u>Fig.35:</u> SEM images of an electronic probe	17
<u>Fig.37:</u> Sketch of the optical circuit used to shine light inside the cortex of the brain [62]	18
<u>Fig.38:</u> Light coupling between two waveguides [64]	19
<u>Fig.39:</u> Working principle of the ring resonators integrated on the optical level of the neural probe [63]	19
<u>Fig.40:</u> Lumerical tests to show the ring resonators transmittance according to the wavelength of the laser used to bring light inside the brain [62]	19
<u>Fig.42:</u> Working principle of the focusing gratings [65]	20
<u>Fig.41:</u> Example of focusing grating [65]	20
<u>Fig.43:</u> Working principle of the focusing gratings [63]	20
<u>Fig.44:</u> Fiber and waveguide dimensions	21
<u>Fig.46:</u> An optical fiber shines light on coupling gratings [65]	21
<u>Fig.45:</u> The two ways to couple a fiber to a waveguide [69]	21
<u>Fig.48:</u> SEM image of the end of the waveguide and of the focusing gratings	22
<u>Fig.47:</u> Fabrication of the optical level of the neural probes	22
<u>Fig.50:</u> SEM image of the electrodes integrated on the shank of the probe	23
<u>Fig.49:</u> Fabrication of the electrical level of the neural probes	23
<u>Fig.51:</u> Back-side etching of the neural probes to define their final thickness	24
<u>Fig.52:</u> Front-side etching of the neural probes to release them	25
<u>Fig.53:</u> SEM pictures of the neural probes. <u>Left:</u> cross section, <u>Right:</u> side-view	25
<u>Fig.54:</u> Microscope image of the neural probe glued on the PCB using Epoxy glue	26
<u>Fig.55:</u> Microscope image of the neural probe glued on the PCB and wire-bonded	26
<u>Fig.56:</u> Silicon neural probe with a focus on the shank on the right picture	28
<u>Fig.57:</u> Oxide neural probe	28
<u>Fig.59:</u> The fiber is approached close to the waveguide to do the alignment and the the fiber gluing	29
<u>Fig.58:</u> Optical set-up to observe the optical components and to glue the fiber on the neural probe	29
<u>Fig.60:</u> Sketch and SEM image of the V-groove etched on the neural probe to ease the fiber gluing	30
<u>Fig.62:</u> Lumerical tests to show the ring resonators transmittance according to the wavelength of the laser used to bring light inside the brain [62]	30
<u>Fig.61:</u> Different ring resonators are shining for different wavelengths	30
<u>Fig.64:</u> Lumerical simulation of the ring resonators transmittance [62]	31
<u>Fig.63:</u> Experimental transmittance of the ring resonators [62]	31
<u>Fig.65:</u> Relative intensity of the luminous spot above the focusing grating according to the distance along the grating for different heights [66]	32
<u>Fig.66:</u> Focusing grating principle [63]	32
<u>Fig.67:</u> Different ring resonators are shining for different wavelengths. Wavelengths from left to right and top to bottom: 449.22 nm, 449.80 nm, 450.30 nm, 450.97 nm, 451.55 nm, 452.13 nm. CCD exposure time = 0.01 ms	32
<u>Fig.68:</u> Representation of the losses of the optical circuit	34
<u>Fig.69:</u> Explanation of the variation of the angle of dispersion when the glue is applied at the interface between the fiber and the waveguide	34
<u>Fig.70:</u> Influence of the glue on the intensity of the focusing grating at the end of the neural probe	34
<u>Fig.71:</u> SEM images of the lens nano-imprinted on the fiber and images showing its influence on the light at the output of the fiber	35
<u>Fig.72:</u> Focusing grating to couple light inside the waveguide from the optical fiber [74]	36
<u>Fig.73:</u> Multi-shank oxide neural probe with an optical circuit on the central shank	36
<u>Fig.74:</u> Recording of neural activity inside a mice's cortex using electrodes integrated on a neural probe [63]	36
<u>Fig.75:</u> RIE principle	41
<u>Fig.76:</u> ICP RIE chamber	42
<u>Fig.77:</u> CCP uses VHF power to boost plasma and RF power to create a DC bias, like and ICP tool [76]	42
<u>Fig.78:</u> Electron-beam evaporator process chamber	43
<u>Fig.79:</u> <u>Left:</u> Original picture showing the focusing gratings shining light. <u>right:</u> The original picture has been modified splitting the channels	44

TABLES

<u>Table 1:</u> Coupling efficiency for the different ring resonators integrated on the shank of the neural probe	31
<u>Table 2:</u> Power extracted from the gratings for the cleaved entrance neural probe	32
<u>Table 3:</u> Power extracted from the gratings for the V-groove neural probe	33
<u>Table 4:</u> Power extracted from the focusing gratings using a nano-imprinted lensed-fiber	35

I) INTRODUCTION

A) Purpose of the report

As a conclusion of the second year of my master's degree focusing on **Nanotechnologies for Information and Communication Technologies**, I had the opportunity to carry out my thesis for **six months** at the **Nano-fabrication Facility of the Molecular Foundry**, one of the lab of the **Lawrence Berkeley National Laboratory (LBNL)**, under the supervision of the **Nano-fabrication Facility Director, Stefano Cabrini**, and of his **PhD student, Vittorino Lanzio**, as a **Research Affiliate**. The *Molecular Foundry* is a lab composed of about **80 staff members**. At the *Molecular Foundry*, there are several facilities dealing with biological or inorganic nanostructures to do both imaging and manipulation of these, but there is also a facility working on the macromolecular and organic synthesis. The topics on which researchers focus in the department are wide and companies are allowed to use the tools available in the laboratories to develop their devices and this for free – under the condition that their research proposal has been accepted. I was working in the Nano-fabrication facility where a cleanroom is available and equipped with state-of-the-art tools (electron-beam lithography, focused ion beam, reactive ion etching, secondary electron microscope, ...) to carry out researches in the micro and nano world.

The project I was involved in focused on **neural probes**, which are micrometric **devices inserted inside the cortex of the brain** for different purposes such as **sensing the Action Potentials (APs)** arising from the communication between different neurons, **delivering chemicals or drugs inside the brain** in accurate areas to study the processes happening at the junction between the neurons or even **stimulate or inhibit some neurons** using light (**optogenetics**) to trigger APs. This report sums up the work that was done during the six months of the internship. It is divided in three parts: first of all, a part deals with the biological background required to understand the functioning of the brain and the interest of the neural probes; a second part focuses on the design and the fabrication steps of the neural probes developed at the *Molecular Foundry*; and in the last part, the results obtained during the internship are shown and further possible improvements are described. My contributions to this project were: doing some of the fabrication steps of the neural probes, mostly the etching parts, and testing the fabricated probes optically.

B) The Lawrence Berkeley National Laboratory (LBNL)

The **Lawrence Berkeley National Laboratory** is a lab depending on the **U.S. Department Of Energy (DOE)** and it is managed by the **University of California (UC)**. More than **3,000 scientists, engineers and staff** are working on site above the San Francisco Bay Area and the Berkeley Campus [2]. It was funded in 1931 by Ernest Orlando Lawrence who won the Nobel Prize in 1939 for his invention of the **cyclotron** [2]. **13 Nobel Prizes worked at the Berkeley Lab** throughout the years which makes this lab known in the research world. The lab is deeply connected with the University of California Berkeley (UCB) because students usually carry out researches or practices there. The UCB is often ranked among the best universities in the world.

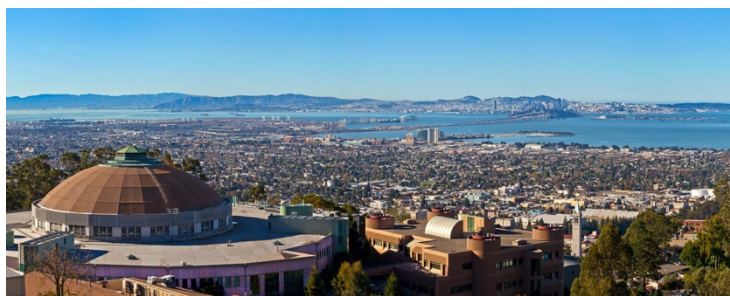


FIG.2: VIEW OF THE CYCLOTRON IN THE FOREGROUND AND OF THE SAN FRANCISCO BAY AREA IN THE BACKGROUND, FROM THE LBNL [2]

II) BIOLOGICAL BACKGROUND AND INTEREST OF A THREE-FUNCTION NEURAL PROBE

The brain and its functioning have always been a source of mystery and of interest for scientists and for humans. The first surgeries on the brain were actually carried out more than five thousands years ago during the Neolithic period by the Egyptians: when some of them were suffering from headaches or mental disorders, it was common to drill or scrap a hole into their skull to try to cure these diseases. Some manuscripts written in 1700BC suggest that Egyptians had some knowledge about the symptoms of brain damage [3]. Although this strong scientific interest throughout the years allowed to understand better some features of the brain such as its internal structures, its composition like the different cells and how they communicate, what part of the brain governs what part of the body, there is still an important lack of knowledge about it and a lot of scientists are nowadays trying to penetrate the mysteries of the brain thanks to the improvements that have been made in the past decades in the micro and nano fabrication technologies. In this part, the functioning of the brain, the way neurons communicate with each other, the goal of drug delivery and finally the working principle of optogenetics are explained.

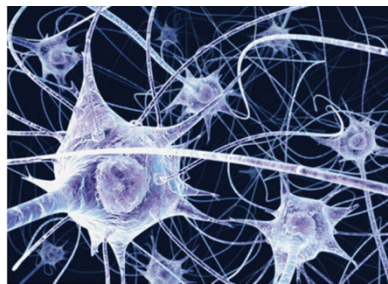


FIG.3: REPRESENTATION OF A NEURON [4]

A) The neurons' communication inside the brain

1) The neurons' structure

The brain is one of the most complex organ in the human body. Its duties include processing the sensory information, regulating the blood pressure and the breathing, which are necessary functions to live. *Galvani*, in 1791, showed on a frog that when a nerve receives an electrical signal, the muscle to which it is connected contracts. This experience proved that electrical signals are an important component of muscles and fibers in the frog's body and so is it in ours. Since then, many discoveries have been made and in the following paragraphs, the neurons' functioning is explained.

The brain is composed of a very high number of cells classified in two categories: the neurons (86 billion in the human brain and the glial cells (85 billion) [5]. Neurons – which are also present in the spinal cord - are the cells allowing humans to move, to think: they are the functional unit of the nervous system and carry action potentials necessary for the communications between the neurons; glial cells have a very important role to play in the brain: they are responsible for providing the nutrients necessary for the neurons to stay alive, they allow to hold physically the neurons, they digest the neurons that are dead and the foreign bodies that could contaminate the brain. The **Fig.4** is an overview of the brain's organization with the different cells.

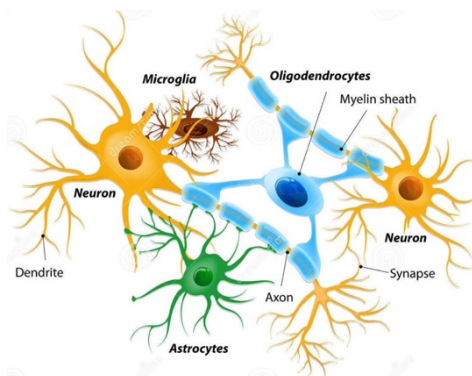


FIG.5: INTERNAL ORGANIZATION OF THE BRAIN WITH THE DIFFERENT KINDS OF CELLS. THERE ARE SEVERAL TYPES OF GLIAL CELLS: OLIGODENDROCYTE, MICROGLIA, ASTROCYTES, EACH HAVING THEIR OWN FUNCTION [6]

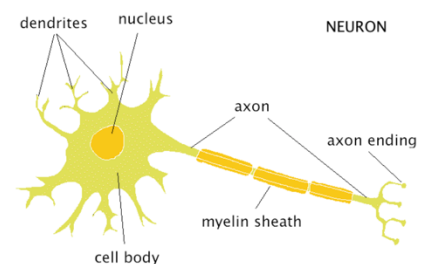


FIG.4: STRUCTURE OF A NEURON [7]

A neuron is a cell whose role is to receive and then transmit some electrical signals in the body. It is composed of three parts, whose representation are given on the **Fig.5**:

- The soma is the place where the nucleus of the neuron containing all the genetics information is held;
- The dendrites are the neuron's branches: they receive chemical and electrical signals from other neurons (many signals can be collected by the numerous dendrites), they are the inputs of the cell;
- The axon is the output of the neuron; it is the connection that allows to transmit the action potentials initiated near the soma from one cell to another.

2) An electrical signal allows for the communication between several neurons

Neurons' communication involves two kinds of signals: one electrical and one chemical. Neurons can first produce Action Potentials (APs) which are electrical pulses: the information carried by the APs flows from the cell body of a neuron towards its axon terminals. APs are due to the opening of voltage-gated ion channels. Basically, when the sum of the stimulus received by one neuron from its dendrites overcomes a certain threshold, an AP will be triggered, as it is shown on the **Fig.6**.

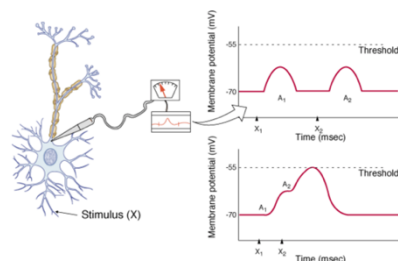


FIG.6: THE ACTION POTENTIAL GENERATION, TEMPORAL SUMMATION [8]

The triggering of an AP is strongly related to the permeability of two ions – Na^+ and K^+ – along the membrane of the axon; the permeability varies according to the different steps of the AP as it is shown on the **Fig.7**.

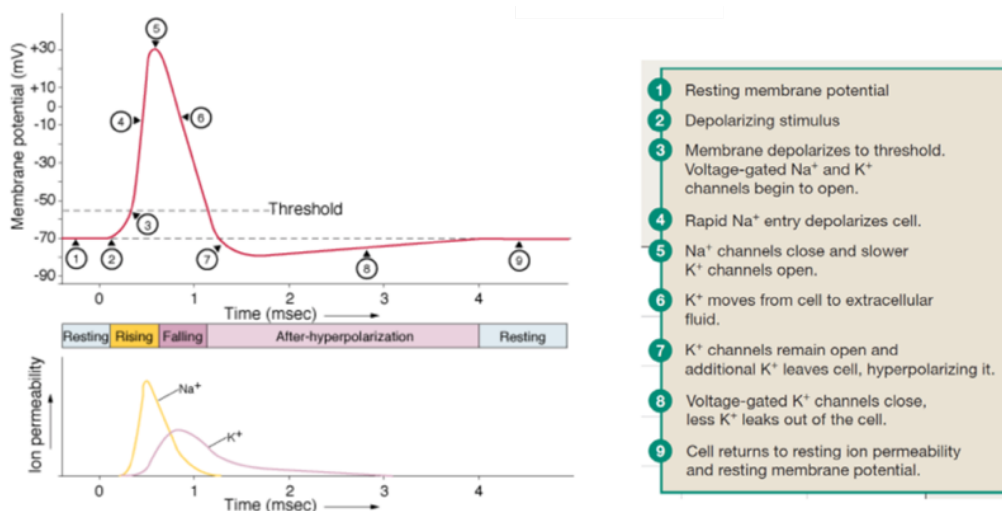


TABLE 8-3 Comparison of Phases of the Action Potential in a Typical Neuron

FIG.7: TIMECOURSE OF AN ACTION POTENTIAL [8]

More details are given on the different steps showing the flows of ions in the membrane (for Na^+) and out of the membrane (for K^+).

During the first step (a), an AP is triggered because the summation of the signals received by the neurons at its dendrites is higher than the threshold voltage (1). Then, the Na^+ channels open up allowing the ions to flow inside the membrane (2), as seen on **Fig.8**.

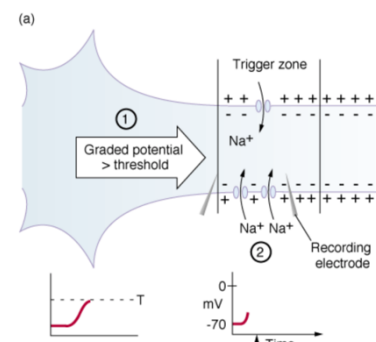


FIG.8: FIRST STEP OF THE AP PROPAGATION [8]

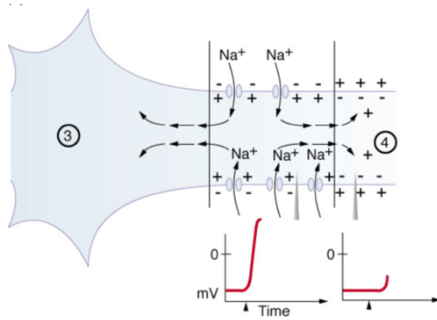


FIG.9: SECOND STEP OF THE AP PROPAGATION [8]

In the last step (c), K^+ ions have allowed to open channels in the region (5) and Na^+ ions cannot trigger any AP in the region (6) because it is refractory (meaning that another AP cannot be triggered if the first one is not finished; the absolute refractory period allows to prevent the back propagation of APs in the cell body). So Na^+ ions initiate APs in the region (7), as seen on [Fig.10](#).

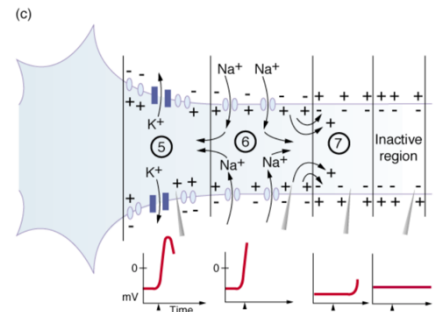


FIG.10: THIRD STEP OF THE AP PROPAGATION [8]

Electrodes could be used to sense the variations of ions' concentrations due to the travel of an AP along the axon allowing to understand better how the neural network is organized inside the brain. Moreover, because the APs are sensed differently at different locations in space (the further the neuron from the recording electrode, the lower the signal), it would be possible to use the signals coming from different electrodes to do a triangulation and to know precisely the location of a neuron to follow the AP propagation along different neurons [9].

3) Translation of the action potential into a chemical signal at the junction between two neurons

When the AP reaches the end of the axon, the pre-synaptic neuron from which the AP originates will communicate with a post-synaptic neuron with a chemical signal: neuro-transmitters, which are ions, are delivered at the junction between these two neurons. The exocytosis is a phenomenon allowing to expel out molecules of the pre-synaptic neuron via an energy-dependent process [10]. These ions will bind to receptors located on the post-synaptic neuron and will trigger a signal in this other cell. The "synaptic" word comes from the fact that the communication between the two neurons is made at the interface between them, called the synapse. There are in average 10^3 synaptic connections for each neuron. The [Fig.11](#) describes in more details how the electrical AP is translated into a chemical signal at the synapse.

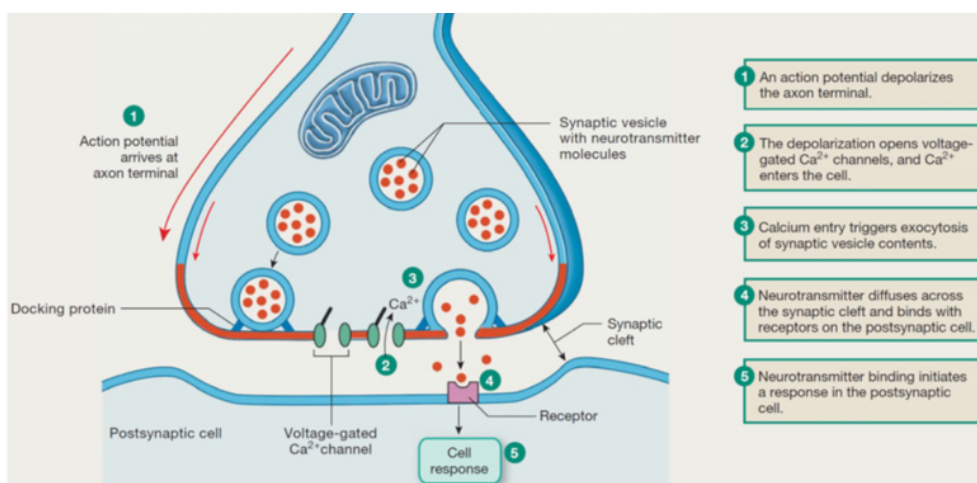


FIG.11: TRANSMISSION OF THE ELECTRICAL AP THANKS TO CHEMICAL NEUROTRANSMITTERS AT THE INTERFACE BETWEEN THE PRE AND THE POST-SYNAPTIC NEURONS [8]

In order to understand the precise role of the neuro-transmitters, the processes happening at the synapses of the neurons and in order to be able to manipulate these junctions, it would be interesting to deliver drugs containing

neuro-transmitters in precise areas of the brain. However, a natural barrier called the Blood-Brain Barrier (BBB) surrounding the blood vessels filters out the molecules that are carried in the vessels and select only the ones essential for the brain; because the neurons are located close to the blood vessels, this barrier also prevent drugs to be delivered at the synapses [11]. Because of this BBB, many diseases cannot be cured because there is no way to cross the barrier even though the drugs to be delivered are already available. Because the variations in the neuro-transmitters concentrations are thought to be responsible for some diseases such as Parkinson's or epilepsy, if it was possible to cross the BBB to deliver drugs near the junction between two neurons, the neuro-transmitters' concentrations could be controlled precisely and therapies for such diseases could be found [12]. It is then extremely important to find a way to deliver drugs in accurate amounts in some regions of the brain and to be able to cross the barrier. Integrating micro-fluidics channels on probes could allow to address this issue of crossing the BBB and deliver drugs in precise areas of the brain.

B) Optogenetics: neural manipulation with light

For years, scientists had noticed the reactivity of some organisms when they were exposed to light, as on the **Fig.12**. Among these organisms, the behavior of algae when exposed to blue light was explained in 2002: researchers from the *Max Planck Institute* in Germany found out that algae were moving away from the light shined on them because of a light-sensitive protein called the channelrhodopsin. The explanation of the behavior of the algae, as seen on the **Fig.13**, is that blue light leads to the opening of ion-gated channels on neural membranes: positive ions then flow inside the cells triggering an AP [13] [14]. Proteins that react to light are called opsins. The science studying the effect of light (optics) on the genes (genetics) is called the optogenetics; this science allows neural cell stimulation by modifying its structure introducing a light-sensitive protein in its DNA to trigger an AP by mean of light.

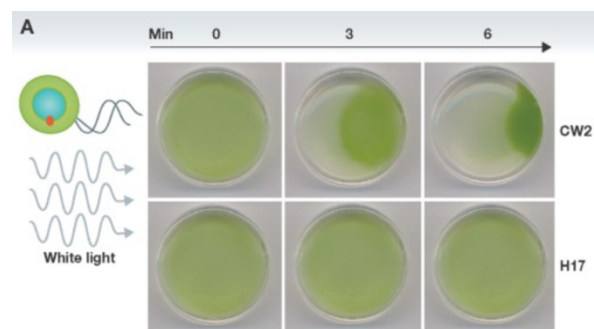


FIG.12: WHEN THE CHANNELRHODOPSIN IS PRESENT IN THE ALGAE (CW2), IT GOES AWAY FROM LIGHT; WHEN THE CHANNELRHODOPSIN IS NOT PRESENT IN THE ALGAE, IT DOES NOT MOVE WHEN IT IS EXPOSED TO LIGHT [15]

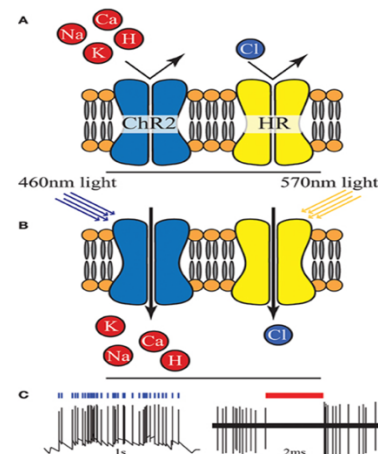


FIG.13: FUNCTIONING OF DIFFERENT OPSINS. (A) THE TWO CHANNEL PROTEINS ARE NOT ILLUMINATED: THEY ARE CLOSED. (B) WHEN ILLUMINATED WITH LIGHT WITH THE RIGHT WAVELENGTH, THE CHANNELS OPEN AND LET IONS FLOW INSIDE THE CELL. (C) ACTIVATION OF CHR2 ALLOWS FOR THE TRIGGERING OF APS WHEREAS HR ACTIVATION SUPPRESSES THE APS [16]

There are several proteins that have been identified as able to react to light: the most used are called the channelrhodopsins (ChR2 mainly), they react to wavelengths centred on 460 nm with a bandwidth of 50 nm [17] and are able to excite neurons triggering an action potential; on the other hand, there are light-reacting proteins able to inhibit neurons like the halo rhodopsin (NpHR), reacting to wavelength around 589 nm [18].

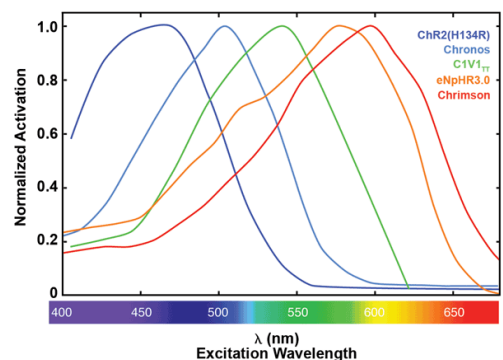


FIG.14: DIFFERENT OPSINS WITH SPECIFIC ACTIVATION WAVELENGTH CAN BE USED [18]

Optogenetics has mostly been explored on mice. To try light activation or light silencing of neurons, mice must be genetically modified in order to have the required opsins that are then activated. Some of the techniques developed up to now are [19] the introduction of opsin genes *in vivo* using recombinant viral vectors (these vectors are used to

deliver genetic materials into specific cells [20]) or the introduction of opsin genes by *in utero* electroporation (during an electroporation, an electric field is applied to some cells making them permeable to outside molecules that can then be inserted in the cell [21]).

On the long-term, optogenetics could be used to cure neuro-degenerative diseases such as Parkinson's, Alzheimer but also depression allowing to activate neurons which are not active anymore [22] [23]. It could even be used to stop seizures by detecting the neurons that are activated during the seizure occurring with recording electrodes and by silencing them using light delivery [24]. It is then important to find a way to shine light inside the brain and manipulate neurons: this can for example be done using an optical fiber inserted inside the cortex.

Up to now, several experiments using optogenetics have been carried out on animals for different purposes:

- Johansen *et al.* have shown that it was possible to control neurons from the lateral amygdala using the protein ChR2 to induce auditory cued fear conditioning [25];
- Using again ChR2, Alilain *et al.* have been able to allow the recovery of the respiratory motor activity on rats with spinal cord injury [26].

C) Comparison between the different brain signals' recording techniques

Understanding the functioning of the neural network requires tools allowing to: record the APs due to the communication between the neurons, deliver drugs in certain areas of the brain to understand the processes happening at the synapses and the role of neurotransmitters, shine light on some neurons to activate or inhibit them. In this part, the interest of the neural probes with respect to other recording techniques is developed.

To record the neural signals inside the brain, there are different technologies available and separated according to their invasiveness: non-invasive techniques make use of tools which are not inserted inside the brain, invasive techniques however make use of tools which are inserted inside the brain. Among the invasive devices, some are called intra-cellular, because they penetrate inside the cells to sense the neural signals, others are called extra-cellular, because the signals are recorded from outside the cells. On the **Fig.15**, the insertion location of several techniques is shown.

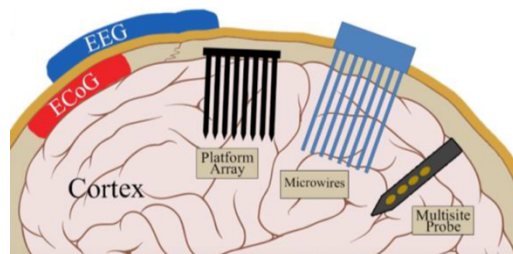


FIG.15: INSERTION LOCATION OF SEVERAL RECORDING TECHNIQUES [27]

Most of the recording techniques are invasive (ECoG, Platform array, microwires, muti-site probe): by introducing them closer to the neurons and below the skull, the signals extracted are less noisy because the skull acts usually as a screen, introducing a lot of noise in the recordings.

Mainly two figures of merit are used to classify the techniques used:

- The spatial resolution: it is the minimum volume from which signals can be recorded;
- The temporal resolution: it is the minimum length of time during which a signal may be measured.

Ideally, researchers want to reach a high spatial resolution, in order to record the neural signals from a lot of neurons to scan a large area of the brain, and a high temporal resolution, to manipulate the neurons with a high speed. The graph below presents the resolutions of several techniques

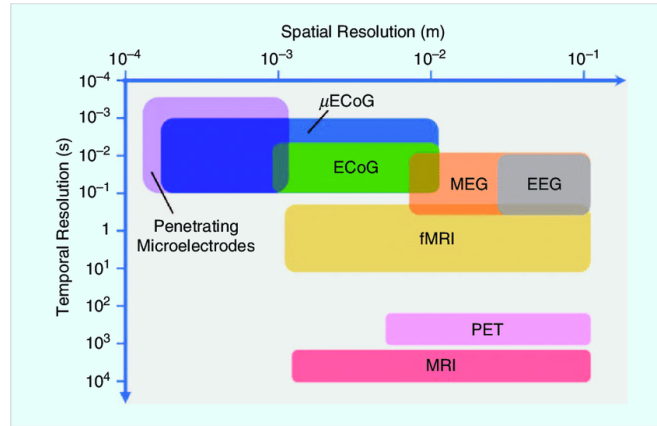


FIG.16: SPATIAL AND TEMPORAL RESOLUTIONS OF SEVERAL RECORDING TECHNIQUES [28]

The different techniques appearing on the **Fig.16** are described:

- ECoG/μECoG (Micro ElectroCorticoGraphy): technique using electrodes placed on the surface of the brain to record electrical activity from the cerebral cortex [29];
- MRI (Magnetic Resonance Imaging): technique using strong magnetic fields, electric fields and radio waves to obtain pictures of the organs in the body [30];
- fMRI (Functional Magnetic Resonance Imaging): measures the brain activity by detecting changes in the blood flow [31];
- PET (Positron Emission Tomography): technique measuring the blood flow in the brain using isotope particles inserted in the blood vessels [32];
- MEG (MagnetoEncephaloGraphy): technique recording the magnetic fields produced by the electrical currents happening in the brain to map the brain activity [33].

Other recording techniques are detailed more in the following.

Non-invasive techniques

ElectroEncephaloGram

The most classic technique to record neural signals is called the ElectroEncephaloGram (EEG), which can be seen on the **Fig.17**. This technique is not invasive because it does not require any surgical operation, it just consists in electrodes that are set on the head of the patient. The electrodes record the voltage fluctuations due to the ionic currents flowing in and out of the cells' membrane when an action potential is triggered. This technique allows to have a high temporal resolution (ms scale) as well as to scan different areas of the brain at the same time. However, the spatial resolution is low (cm scale) [35] and the signal-to-noise ratio is reduced because the area of the recording electrodes is large and because the skull acts as a screen and reduces the amount of signal that can be sensed.

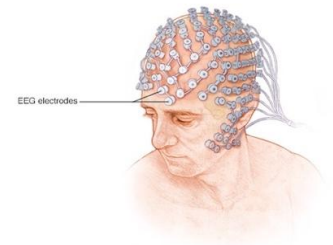


FIG.17: EEG PRINCIPLE [34]

Multi-Electrodes Arrays (MEA)

Another technique to record electrical potentials relies on the Micro-Electrodes Arrays: they are flexible arrays of electrodes made with polymers, like polyimide or parylene. They are not implanted inside the brain and are usually used *in-vitro*, this however limits their resolution because recording electrodes are far away from neurons.

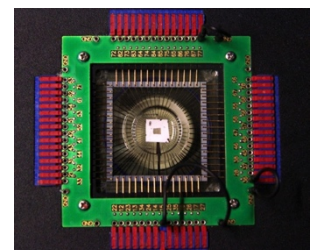


FIG.18: MEA STRUCTURE: THE ELECTRODES ARE LOCATED AT THE CENTER OF THE SQUARE [36]

The other techniques that are being developed nowadays rely on the implantation of devices inside the brain: they are invasive techniques because they penetrate the brain tissue allowing to improve the quality of the recorded signals thanks to the higher proximity with the neurons. These techniques are further described.

Invasive techniques

Microwires

Microwires are very thin devices made of insulated metallic conductors. Their diameter is on the order of a few tens of microns. The tips of these wires are not insulated so that they can sense the neural signals translating the variation of ions near the cell's membrane into an ionic current carried by electrons. Thanks to the sharpness of the tip, insertion in the brain is easy. However, a trade-off must be found between the material used for the electrodes (to have a high bio-compatibility and reduce the inflammatory response of the body after insertion) and the tip shape (to ease the insertion of the microwires inside the cortex). The [Fig.19](#) shows microwires developed by [37].

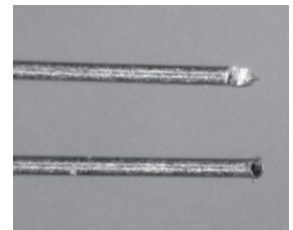


FIG.19: MICROWIRES TIP NOT INSULATED [37]

Multi-functional fibers

Seongjun Park *et al.* have developed polymer-based fibers, close to the microwire design, including three functionalities: they are integrated with one optical waveguide to shine light in the brain, two micro-fluidic channels to deliver drugs in the brain and six electrodes to record the electrical signals in the brain [38]. In order to develop the electrodes, they managed to create a hybrid polymer to increase the electrodes conductivity thanks to graphene. An image of the result is shown on the [Fig.20](#). These probes have been successfully implanted in mice; activation of ChR2 channels has been carried out thanks to the optogenetics technique.

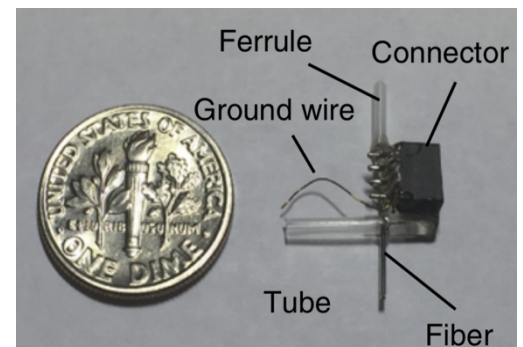


FIG.20: PICTURE OF A MULTI-FUNCTIONAL FIBER [38]

Neural probes

Another technique relies on the neural probes which are devices on which electrodes and other components are integrated. These probes are inserted inside the cortex of the brain to record the neural signals, to deliver drugs near the synapses or to shine light on some neurons to manipulate them. Using neural probes allows recording signals from a single neuron because the probes are inserted close to the targets and because the size of the electrodes integrated on the probe is on the order of a neuron's diameter (tens of microns). However, this technique is highly invasive because the probes are inserted inside the brain tissue.

Among the neural probes, there are two types of devices: one is called the Utah probe – consisting in arrays of vertical probes, the other one is called the Michigan probe – consisting in probes fabricated by successive depositions of layers. An illustration of these neural probes is given on the [Fig.21](#) and [Fig.22](#) respectively.

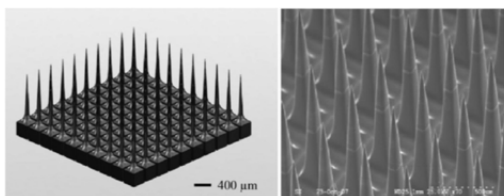


FIG.21: UTAH-TYPE PROBE [23]

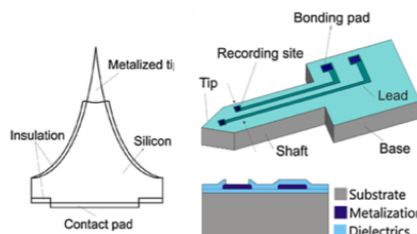
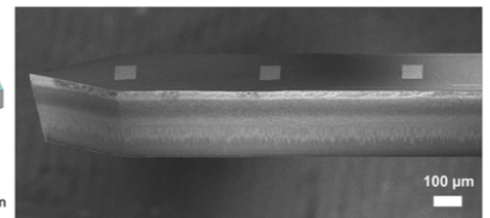


FIG.22: MICHIGAN-TYPE PROBE [23]



The two probes presented above may include different functionalities (electrical, optical and fluidic) and are low-cost because they can be fabricated reliably and with a high throughput taking advantage of the micro and nano fabrication techniques. For what concerns the Utah-type probes, the main limitation is correlated with their fabrication: because these probes rely on micromachining techniques, their length is limited by the thickness of the silicon wafer (the longest probe length reported is 1.5 mm [39]) while to carry out measurements on the human brain, a probe of 3 to 4 mm is required to reach all the layers of the cortex; moreover, only one electrode can be integrated on each probe which limits its recording capability [40]. However, they have already been used for

recording electrical signals on humans. On the other hand, Michigan-type probes allow to reduce the damages to the brain thanks to their lower thickness [23]. They also allow to integrate a high-density of electrodes on the same probe - thanks to the electron-beam lithography which allows to reduce the width of the wires used for the electronic connections – and other functionalities for optical and fluidics applications.

The way electrodes are integrated on the invasive tools explained above to sense neural signals can be explained as follows: when an AP is triggered, ions flow in and out of the cells' membrane inducing a change in voltage between the inside and the outside of the cell: this change in voltage is translated into a current carried by electrons on the electrodes of the devices to measure the APs.

In order to sense this phenomenon, the model on the **Fig.23** has been elaborated. This model is valid for extracellular recording techniques i.e. when the recording device is not inserted inside the neuron. This is the case for the techniques presented previously.

On the **Fig.23**, there is an ionic solution between the neuron (light blue) and the recording electrode (orange) fabricated on the substrate (yellow). This ionic solution contains the ions which can flow inside the membrane when the channels open up after an action potential: this part is called the cleft. The part of the membrane facing the electrode is called the junctional membrane (dark blue)

and is represented by the junctional membrane resistance R_j and the junction membrane conductance c_j . The other part of the membrane, called the non-junctional membrane (red), is represented by a non-junctional membrane resistance R_{nj} and a non-junctional membrane conductance c_{nj} . The ionic solution between the neuron and the electrode generates the seal resistance R_{seal} . The electrode impedance is represented by a resistance R_e and a capacitance c_e . The electrode can either be a transistor or a passive element [41].

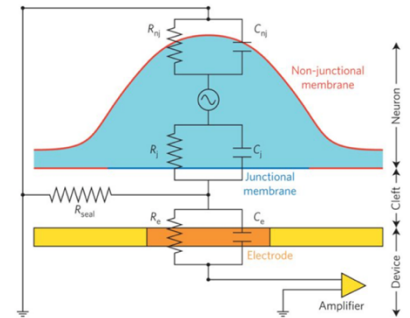


FIG.23: SKETCH SHOWING THE SPATIAL RELATIONSHIPS BETWEEN A NEURON AND A SUBSTRATE-INTEGRATED ELECTRODE AND THE ANALOGUE PASSIVE ELECTRICAL CIRCUIT [41]

The electrodes integrated on the microwires or neural probes are passive components. However, with the development of the CMOS technology, more complex components have been developed and integrated on the neural probes: several papers have demonstrated the possible use of transistor-based probes to record the electrical signal. In [42], a NanoWire integrated with Field Effect Transistors (NWFET) has been successfully used to record neural signals. Basically, the drain current of the transistor is modified when an AP is triggered by a neuron because the gate, which is in proximity with the neuron, sees its voltage changing. The NWFET are advantageous because they allow to detect one single neuron.

Neural probes allow to integrate a very-high density of components for manipulating the neurons inside the brain and then to read the neural signals due to the stimulations. They allow to get the highest spatial (μm scale) and temporal (ms scale) [35] resolutions with respect to other techniques because they can integrate a high density of electrodes and because using optogenetics allows to manipulate neurons at a very high speed in the cortex of the brain. However, this technique is invasive and long-term stability and recording-capability of the device may be limited due to the inflammatory response of the body when the probe is inserted inside the brain. Indeed, after the insertion of the probe inside the cortex, glia cells develop around the probe, preventing the recording of signals [43]. Also, with respect to EEG, neural probes allow to interface only one area of the brain at a time. The neural probes developed at the *Molecular Foundry* are of the Michigan type.

D) What parameters must be taken into account when developing a neural probe?

When trying to develop neural probes, there are important parameters that must be taken into account:

- **Multi-functionality:** to understand how the neural network is organized and to find therapies for neuro-degenerative diseases, probes must integrate components allowing two main functions at the same time: stimulate the neurons in order to activate/silence them: this is the role of the optical components integrated to shine light inside the brain, and of the micro-fluidic channels which allow to deliver drugs inside the brain; and the neural signals generated by these stimulations must be sensed: this is the role of the electrodes integrated on the probes. This multi-functionality allows to stimulate certain areas of the brain and then to get feedback loops to read the neural network;

- High-density: in order to read signals coming from a lot of neurons at the same time, it is important to integrate many electrodes on the probes [44];
- Biocompatibility: when a probe is inserted inside the brain, the immune system reacts to the insertion because the probe is seen as a foreign body. The reaction induced by the immune system leads to the encapsulation of the probe by glia cells, which increases the distance between the electrodes surface and the neurons preventing good signal recordings and long-term stability of the probe [45]. Thus, it is important to reduce as much as possible the reaction of the immune system by selecting materials with a Young's modulus close to the brain's one. Silicon and metals have Young's modulus of 190 GPa and 78 GPa respectively, whereas dura mater (membrane made of connective tissue surrounding the brain and the spinal cord to protect them, between the cranial bone and the cortex) and cerebral cortex range between 0.4 MPa - 1.2 MPa and - 0.03 - 1.75 kPa for the rat, explaining why the inflammatory response of the immune system can be important [46]. To solve this issue, polyimide-probes have been investigated (Young's modulus between 2.3 GPa and 8.5 GPa) and have successfully recorded signals in rat's brain [47]. Some researchers have also used organic transistors to record the electrical signals: these organic transistors help to meet the required biocompatibility [48]. Silicon is very often used because nano-fabrication techniques are well-known for this material even though its Young's modulus does not make it biocompatible (180 GPa). Also, in order to limit the inflammatory response of the body after the insertion of the probe inside the cortex and to limit the encapsulation of the probe by the glia cells, the dimensions of the probes must be reduced;
- Mechanical strength: in order for the probes not to break during the insertion and the retraction phases inside the brain, which both induce a lot of stress, they should be stiff enough and strong mechanically to penetrate the dura of the brain [49]. Using Silicon-based neural probes usually allows to penetrate inside the cortex of the brain without breaking due to the high Silicon Young's modulus; however, when polymeric probes are developed, their high flexibility implies the need of a customized implementation mean in order to penetrate the dura mater. To improve the stiffness of the polymeric probes, a bio-degradable coating can be used just for the insertion phase, for example Parylene-C, that is then dissolved in the brain in as fast as 200 seconds. Another solution is to use a shuttle (tungsten push rod) to help the insertion inside the brain: this rod is then removed after the insertion [46].

E) State-of-the-art for the Michigan neural probes

The first Michigan probes were developed by *Wise and his colleagues* at the *Michigan University* in 1981. Since that date, researchers have tried to develop smaller probes, with a higher density of recording sites and integrating more functionalities. In this part, some of the best results achieved so far are shown.

Concerning the high-density of recording electrodes, a 10 mm long probe called *Neuropixels* developed by *James J. Jun et al.* [50] has 96 sites per mm which allow to record signals coming from many neurons at the same time (there are 384 channels available at the same time to carry the signals). In the article, the authors report that using two probes in a mice brain, more than 700 single-neuron signals have been recorded at the same time. Despite the high number of electrodes, the probes' dimensions remain small: the cross-section of the probe is only 20 μm x 70 μm . The probe base also integrates electronic active components such as amplifiers, multiplexers to deliver a noiseless signal from the probe.

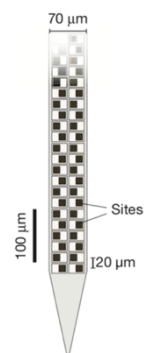


FIG.24: HIGH-DENSITY NEURAL PROBE [50]

Concerning the delivery of chemicals in the brain using micro-fluidic channels, a probe developed by *Demetrios Papagiorgiou et al.* [51] is integrating three micro-fluidic channels, each having one hole to release the chemicals inside the brain; apart from these orifices, shutters have also been developed to open or close the micro-fluidic channels and flowmeters measure the exact amount of drugs delivered. A few electrodes are also present on the probes to record the electrical signals. This probe demonstrates a high degree of integration of fluidic components.

An application for drug delivery has been exposed by *Hyunjoo et al.*: this team has successfully produced a double-functionality neural probe (integrating both micro-fluidic channels and electrodes) and they have been able to first record

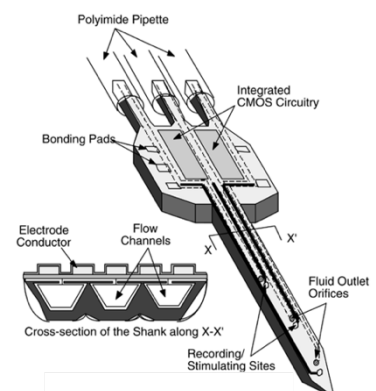


FIG.25: NEURAL PROBE WITH MICRO-FLUIDIC CHANNELS FOR DRUG DELIVERY INSIDE THE BRAIN [51]

neural signals showing an activity of the neurons due to a seizure and then to stop it by delivering Baclofen thanks to the micro-fluidic channels, which is a drug able to inhibit the firing neurons. The results are shown on the **Fig.26** and **Fig.27**.

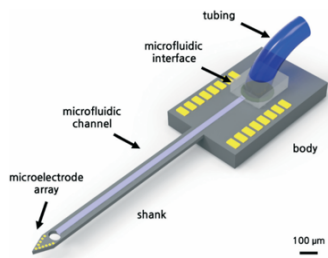


FIG.27: DOUBLE-FUNCTIONALITY NEURAL PROBE: ELECTRODES AND MICRO-FLUIDIC CHANNELS [52]

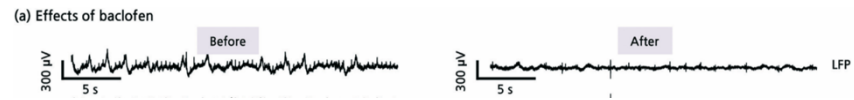


FIG.26: MEASUREMENTS SHOWING THE EFFECTS OF THE DRUG DELIVERY INSIDE THE BRAIN: THE ACTION POTENTIALS DUE TO THE SEIZURE ARE REDUCED WITH BACLOFEN [52]

Concerning the optical part, a recent article is reporting tests on mice with an optoelectronic probe [53]. This probe integrates 20 recording electrodes and 1 waveguide per shank (the part of the neural probe inserted inside the cortex of the brain). The waveguide has three directional couplers and the light is radiated thanks to gratings. The probes are 5.2 mm long and 100 μm wide. The electrodes are 20 μm x 20 μm which make them suitable for single-neuron recording, because the diameter of a neuron is on the order of 10 to 20 μm. The gratings and the electrodes have been successfully used on mice to stimulate optically the neurons and then record electrical signals. However, this probe does not allow to select the area of the brain that is illuminated because gratings are all shining light at the same time: this issue could be solved using ring resonators, as it will be seen in **III)A)2)**.

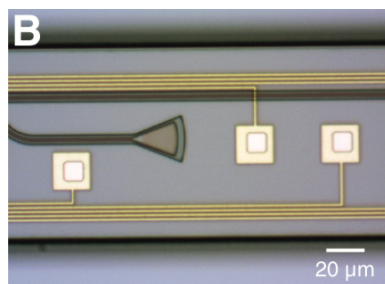


FIG.29: OPTOELECTRONIC PROBE COMBINING ELECTRODES AND GRATINGS TO STIMULATE NEURONS AND RECORD THE INDUCED ELECTRICAL SIGNAL [53]

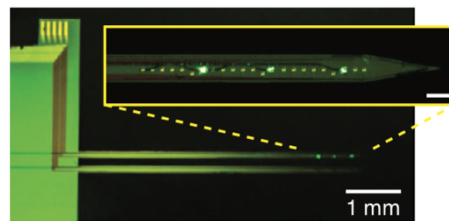


FIG.28: THE GRATINGS OF THE PROBE ARE RADIATING LIGHT [53]

Another solution to shine light inside the brain relies on micro LEDs: these light sources are directly integrated on the probe thanks to nano-fabrication techniques. According to [54], the integration of LEDs on the probe allows for a very efficient coupling into the brain tissue. It is also easier to match the stimulation zone with the light and the recording zone with electrodes. However, because LEDs' efficiency is highly dependent on the defects' density, the materials that can be used and so the wavelengths that can be radiated in the cortex are limited: not all opsins can be activated. Also, the electrical power is dissipated as heat at the surface of the LEDs which has two consequences: this may damage the brain tissue and influence neuron's behavior - as they are sensitive to thermal fluctuations - or even kill them [55].

Despite these issues related to LEDs properties, a work carried out by [56] is presented **Fig.30**. This group has been able to develop a probe integrated with 12 micro LEDs and 32 recording sites while limiting at the same time the heat generated by the optical components. This probe was successfully tested on mice: stimulation with light has been done and signals post-stimulation have been sensed too allowing to control a distinct cell at a distance of 50 μm.

Currently, from the best of our knowledge, there is no neural probe combining at the same time optics, microfluidics and electronic functions: our goal is to address this challenge.

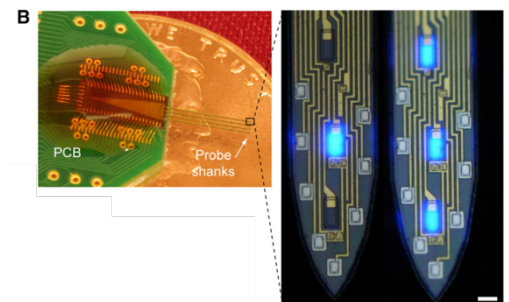


FIG.30: NEURAL PROBES INTEGRATED WITH MICRO LEDs TO SHINE LIGHT INSIDE THE CORTEX [56]

III) THE MICHIGAN PROBES DEVELOPED AT THE MOLECULAR FOUNDRY

As explained before, the goal of the project is to develop a Michigan neural probe integrating the three following functionalities: electrodes to be able to record the neural signals such as the APs, waveguides to be able to shine light inside the brain to activate groups of neurons, micro-fluidic channels to be able to deliver drugs inside the brain.

A) Probes' structure and design

The neural probes developed at the *Molecular Foundry* are divided in two parts: the shank, which is the part of the probe inserted inside the cortex of the brain and which contains all the components required for recording the neural signals and for manipulating the neurons, and the bonding area, which allows to interface external components such as electronic circuitry or an optical fiber. These two parts can be seen on the [Fig.32](#).

The shank of the probe is 1 mm long, 45 μm wide, 15 to 25 μm thick. The cortex of the brain, where the shank is inserted, is divided in different layers in which a specific type of neuronal cell is present; these cells are connected to each other thanks to nervous fibers [57]. The length of the shank has been chosen in order to reach the different layers of the cortex of the mice's brain. The dimensions aim also at reducing the inflammatory response when the probe is inserted in the brain [58].

To interface the probe and the external environment, a Printed Circuit Board (PCB) is used to connect the neural probe and the data treatment tools located outside the brain: the pads of the bonding area of the probe are connected to the PCB thanks to an automatic wire-bonding tool using gold or aluminum wires. The [Fig.31](#) and [Fig.32](#) show the structure of the probe and the interface with the PCB.

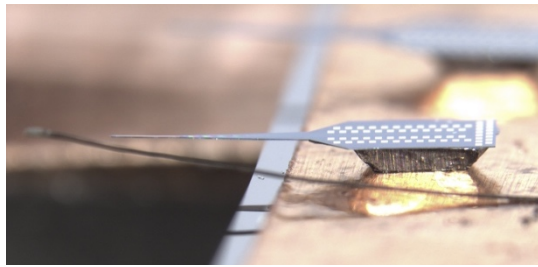


FIG.31: PICTURE SHOWING THE STRUCTURE OF THE PROBE COMPARED WITH A HAIR

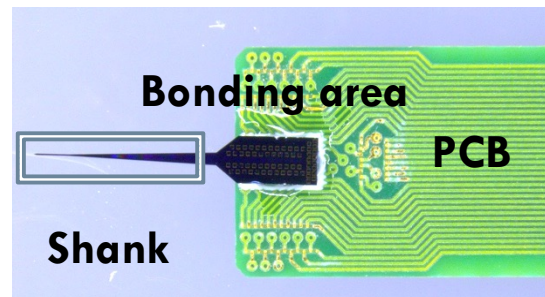


FIG.32: PROBE GLUED ON THE PCB USING EPOXY GLUE, BEFORE THE WIRE-BONDING

The sketch [Fig.33](#) shows how probes are inserted in the brain: after a craniotomy (the neuroscientists dig a hole in the skull), the probes are inserted through the dura mater and then reach the cortex where the signals can be recorded. The PCB and a long part of the probe are out of the mice's brain: only the shank and the tip (end of the shank) are penetrating inside the cortex.

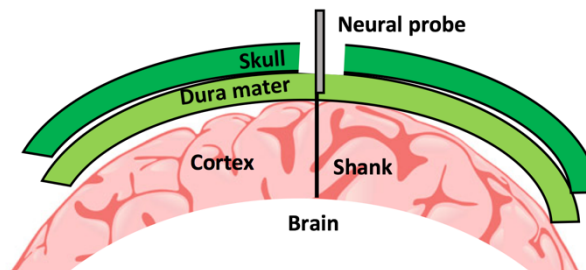


FIG.33: SKETCH OF A PROBE INSERTED INSIDE THE CORTEX OF THE BRAIN

The probe's shank is divided in two different levels: the lower one includes optical components (waveguide, ring resonators and gratings) to shine light inside the brain while the upper one includes electrodes to record neural signals. These components will be detailed further. The sketch [Fig.34](#) gives an idea of the shank of the probes developed at the *Molecular Foundry*.

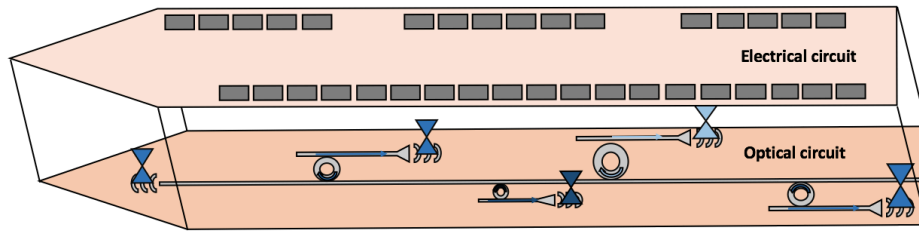


FIG.34: SKETCH OF THE 2-LEVEL SHANK DEVELOPED UP TO NOW: THE LOWER LEVEL IS COMPOSED OF OPTICAL COMPONENTS FOR OPTOGENETICS, THE UPPER ONE IS COMPOSED OF ELECTRODES TO RECORD THE NEURAL SIGNALS

A 4 inches Lionix TriPleX wafer was chosen to be the base structure of the probe. This wafer is made of a Silicon substrate (525 μm) sandwiched on both sides by a layer of SiO_2 (2.5 μm deposited thermally) and on top of it, a high quality layer of Si_3N_4 (160 nm deposited with Low Pressure Chemical Vapor Deposition (LPCVD)). The Lionix TriPleX wafers are preferred with respect to SOI wafers because they allow low level of stress as well as a high optical quality, required for the photonics circuit of the probes [59].

1) Electrical part

In order to be able to record signals from a lot of neurons with a single neuron resolution, it is important to be able to integrate a lot of small electrodes on the neural probes. There are 64 electrodes integrated per shank, made of a layer of gold (100 nm) evaporated on top of a layer of titanium (10 nm) to improve the adhesion of gold. Gold has been chosen because it has a low resistivity. The electrodes dimensions are 5 μm x 25 μm , and they are separated by 2.5 μm . These dimensions allow to sense the signals coming from only one neuron for each electrodes because the diameter of a neuron ranges from 10 μm to 20 μm . Using smaller electrodes would lead to an oversampling, i.e. one neuron would be sensed by two electrodes. However, oversampling can be useful to allow to sort the electrical spikes recorded due to the APs when triangulation of neurons is required [60].

The electrodes are connected to pads on the bonding area using gold wires that are 110 nm thick (in the shank only to allow a high density of integration with a limited width), 120 nm wide (in the shank only to allow a high density of integration with limited width), 10 mm to 12 mm long and their pitch is 100 nm. These pads are used to connect the probe to the PCB and are 100 μm x 100 μm . These components are seen on the [Fig.35](#) and [Fig.36](#).

Because the optical circuit used to shine light inside the brain is inserted below the electrical level, when light is focused, it may be scattered by the gold electrodes and wires integrated on the upper level. To prevent this issue, the width of some electrodes has been reduced and wiring has been done in such a way that it does not overlap with the components of the optical circuit.

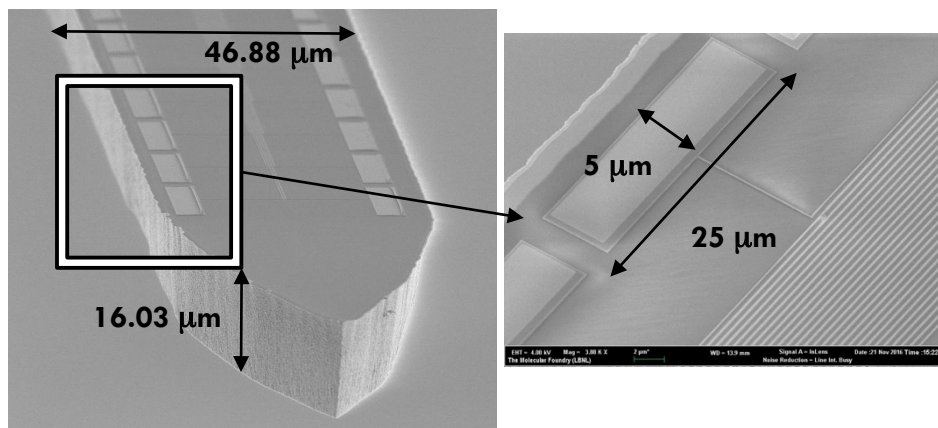


FIG.36: SEM IMAGES OF AN ELECTRONIC PROBE

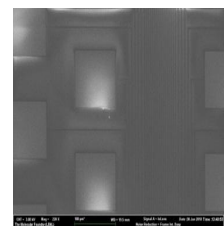


FIG.35: SEM IMAGES OF THE PADS OF THE BONDING AREA

2) Optical part

The goal of the optical components integrated on the probes is to shine light in different and precise areas of the brain to activate or inhibit specific neurons. Waveguide photonics has been preferred with respect to micro LEDs because they allow to develop more complex shapes of optical circuits in order to directly integrate components used to select in which area of the brain the light will be shined; also, they allow to use different wavelengths in order to

activate different opsins at the same time using light splitter and to cancel the heating issues due to the dissipation of power which occurs with the LEDs.

Light is carried on the shank thanks to a waveguide made of Si_3N_4 ($n = 2$) surrounded by SiO_2 ($n = 1.45$): these materials have been chosen because they have low light absorption in the visible range corresponding to the wavelengths used to active or to inhibit the opsins. Indeed, for Si_3N_4 waveguide, losses below 1 dB/cm have been reported in [61].

On the shank of the probe, 4 to 5 ring resonators are integrated to couple light into different branches according to the wavelength of the light. To extract light from the waveguide in which the light has been coupled from the ring resonators, focusing gratings are integrated at the end of each branch as well as at the end of the main waveguide. These gratings focus the light within a $1\ \mu\text{m}$ spot at a distance of $20\ \mu\text{m}$ from the shank's plan. The **Fig.37** shows the optical circuit integrated on the shank.

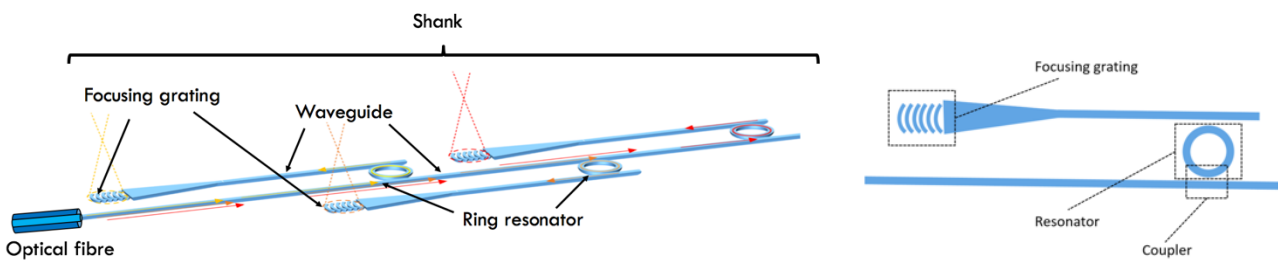


FIG.37: SKETCH OF THE OPTICAL CIRCUIT USED TO SHINE LIGHT INSIDE THE CORTEX OF THE BRAIN [62]

The optical components are developed thanks to electron-beam lithography, dry etching using the Reactive Ion Etching (RIE) of Si_3N_4 and the deposition of SiO_2 ($2.5\ \mu\text{m}$) using Plasma-Enhanced Chemical Vapor Deposition (PECVD). The electron-beam lithography is used to allow a high density of integration of optical components. Depositing a layer of SiO_2 allows to insulate the optical and the electrical layers of components and to prevent the scattering of the light from the waveguide with the gold used for the electrodes and wires. More details are given for the components further.

a) Waveguide

The waveguide developed on the probe is $300\ \text{nm}$ wide and $160\ \text{nm}$ high: its width has been optimized with Lumerical - knowing that the height is fixed by the Lionix TriPleX wafer - in order to have a single-mode propagation for blue light centered on $450\ \text{nm}$ [63]. The blue light corresponds to the one used to activate the ChR2 opsin, one of the most used in optogenetics studies. This waveguide goes from the bonding area of the probe until almost the end of the shank (it is between $750\ \mu\text{m}$ and $900\ \mu\text{m}$ long).

This waveguide is single-mode: this is a requirement for the ring resonators to trap light with a high efficiency. Indeed, to have a good selection of the wavelength that is trapped inside the ring resonators, they require coherent and single-mode light with a narrow spectral bandwidth.

The waveguide entrance, located on the bonding area of the probe, is tapered (enlarged) to $4\ \mu\text{m}$ in order to allow a good mode-matching with the core of the fiber used to bring light inside the brain (*cf. explanation in III)A)2)b)*), which has a $4\ \mu\text{m}$ diameter. In order to filter the unwanted modes of the light, the width of the waveguide is then reduced to $250\ \text{nm}$ before being increased again to the final $300\ \text{nm}$ width.

The output waveguides to which the ring resonators are coupled are also tapered at the output, before the gratings. This allows to develop focusing gratings which are not too narrow: if the focusing gratings were too narrow, they would reduce the light out-coupling i.e. the light they can extract from the waveguide and lead to a large light spreading which would not be compatible with focusing the light in precise areas of the brain. Also, if the gratings were narrower, their height should be increase to keep the same efficiency which would not be possible because the height of the Si_3N_4 layer is fixed by the Lionix TriPleX wafer.

b) Ring resonators

The ring resonators integrated on the shank of the neural probes work as ON/OFF switches for the light that is traveling in the central waveguide, meaning that they allow to trap the light from the waveguide when the wavelength of this light is a multiple of the ring diameter ($\lambda_{\text{resonance}} = n_{\text{eff}} \cdot L/m$, where $\lambda_{\text{resonance}}$ is the resonance wavelength of the ring, n_{eff} is the effective refractive index, L is the ring circumference). This trapping of the light

happens thanks to the coupling between the central waveguide and the ring resonator, meaning that there is a transfer of energy between these two waveguides when the light travels in the central waveguide of the shank, as seen with two linear waveguides on the **Fig.38** [64].

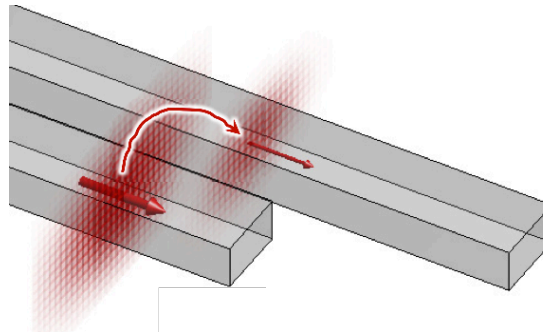


FIG.38: LIGHT COUPLING BETWEEN TWO WAVEGUIDES [64]

The ring's functioning is detailed on the **Fig.39**.

- When the light wavelength matches the ring resonance wavelength, the light is trapped in the ring and coupled in the top waveguide;
- When the light wavelength does not match the ring resonance wavelength, the light is not trapped in the ring and remains in the same waveguide (bottom one).

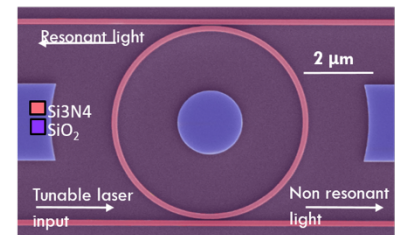


FIG.39: WORKING PRINCIPLE OF THE RING RESONATORS INTEGRATED ON THE OPTICAL LEVEL OF THE NEURAL PROBE [63]

The opsins that must be activated have an absorption curve on the order of 50 nm as it can be seen on the **Fig.14**. In order to select which area of the cortex of the brain is illuminated, the ring resonators developed on the shank have different diameters, allowing them to couple distinct wavelengths while remaining in the range of activation of the opsins used (in our case Chr2). Doing so allows to trap light in different ring resonators for specific wavelengths, as it can be seen on the **Fig.40** where Lumerical® simulations give the ring transmittance according to the light wavelength. The Full Width at Half Maximum (FWHM) of the curves has been chosen to match with the Q factor of the tunable-wavelength laser that is used to bring light inside the central waveguide of the neural probe.

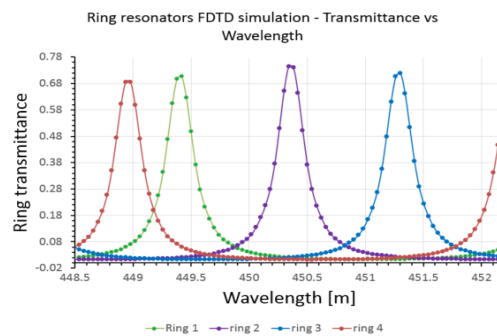


FIG.40: LUMERICAL TESTS TO SHOW THE RING RESONATORS TRANSMITTANCE ACCORDING TO THE WAVELENGTH OF THE LASER USED TO BRING LIGHT INSIDE THE BRAIN [62]

So by trapping the light in different ring resonators using a tunable-wavelength laser connected to the central waveguide and by then coupling this light to an output waveguide, it is possible to select in which area of the brain the light will be focused.

The gap between the center of the main waveguide and the center of the ring resonators waveguide determines the distance between the mode of the light: the smaller the gap, the higher the overlap between the waveguide and ring's wavefunctions and so the higher the coupling efficiency [62]. The optimized gap between the two waveguides' sides has been determined as 30 nm for a blue wavelength (450 nm) [63], for a waveguide width and height of 320 nm and 160 nm respectively and for a ring diameter of 3.1 μm [63]. However, due to the limits of resolution due to the etching of the Si₃N₄ layer with the RIE, the best gap obtained is on the order of 80 nm to 90 nm but the distance

between the centers of the central waveguide and of the waveguide of the ring remains the same which allows still a good light coupling between the two waveguides.

c) Gratings

Gratings are periodic structures that are defined on or in a Silicon waveguide, as it can be seen on the **Fig.41** and **Fig.42**. These structures allow to diffract light in different beams due to the scattering centers located at the interface of the slits and tooth of the gratings [65]. These beams will then interfere due to the specific phase relation because of the periodicity of the structure. Depending on the angle of incidence of the light to be scattered and on its wavelength, depending also on the pitch between the gratings and on their shape, light can be focused at different angles for the different diffraction orders.

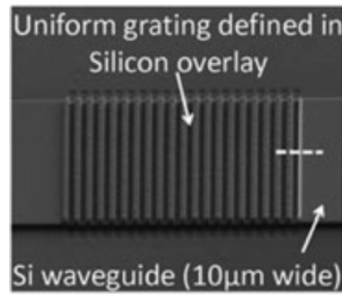


FIG.42: EXAMPLE OF FOCUSING GRATING [65]

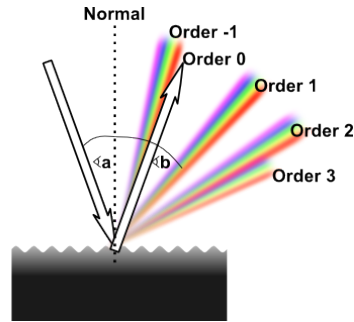


FIG.41: WORKING PRINCIPLE OF THE FOCUSING GRATINGS [65]

The output optical components of the probe are curved focusing gratings. They are $4 \mu\text{m}$ wide and $10 \mu\text{m}$ long. Each grating extracts light by diffraction from the waveguide in which it was coupled from the ring resonator; the light is extracted in a conical shape as it can be seen on the **Fig.43**.

The intersection of all the diffracted light-rays corresponds to the focal point, which is located $20 \mu\text{m}$ above the plane of the gratings within a $1 \mu\text{m}$ spot diameter [66]. This spot of light, used to manipulate the neurons, must be located far from the probe's shank because when the probe is inserted inside the brain, the neurons around the insertion zone are killed: the goal is then to reach the neurons further from the insertion zone.

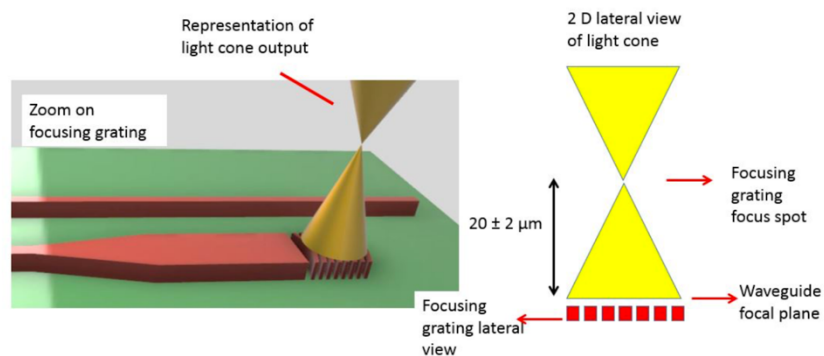


FIG.43: WORKING PRINCIPLE OF THE FOCUSING GRATINGS [63]

d) Bringing light in the central waveguide using an optical fiber connected to a laser

Once the photonics circuit is fabricated, an external component is required to bring light inside the central waveguide; this light is then coupled to ring resonators and focused in the cortex using the gratings. In order to bring the light in the central waveguide, a tunable-wavelength laser can be connected to an optical fiber which is then coupled to the waveguide.

A high coupling efficiency is required between the fiber and the waveguide to reduce the losses at the interface which, if too high, would require the use of very powerful laser to reach the threshold of activation of the opsins (power density required on the order of 0.1 mW/mm^2 [67] to 1.1 mW/mm^2 for the ChR2 opsin [68]).

In order to reach a high coupling efficiency between the fiber and the waveguide, i.e. to have most of the light from the fiber's core transferred in the waveguide, the overlap between the two wavefunctions must be high: this is done by matching the dimensions of the core of the fiber and the ones of the waveguide. Indeed, the entrance of the waveguide is tapered (enlarged) to 4 μm match with the fiber's core diameter to reach a higher coupling efficiency. The dimensions of the waveguide and of the fiber are shown on the [Fig.44](#).

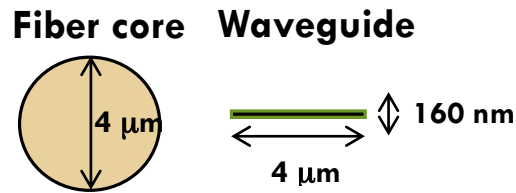


FIG.44: FIBER AND WAVEGUIDE DIMENSIONS

There are two different techniques that can be used to couple the fiber to the waveguide: the edge-coupling and the grating coupling, these techniques are presented on the [Fig.45](#) (the image on the left shows a non-tapered waveguide but the design for the neural probes has one).

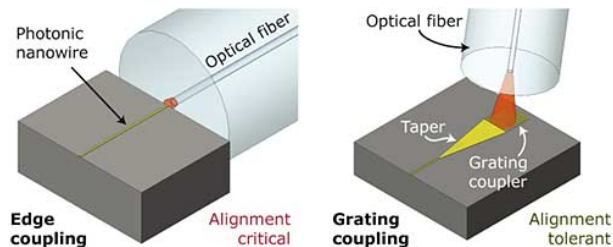


FIG.46: THE TWO WAYS TO COUPLE A FIBER TO A WAVEGUIDE [69]

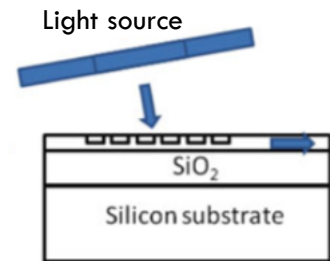


FIG.45: AN OPTICAL FIBER SHINES LIGHT ON COUPLING GRATINGS [65]

The first solution is to do an edge-coupling between the fiber and the waveguide: the fiber is aligned horizontally with the waveguide and brought in close proximity using micro-manipulators because a high precision is required to reach a high coupling efficiency.

The other solution is to use a grating coupler: optical structures similar to the ones that are used to focus the light inside the cortex of the brain are etched on the device and allow to diffract the light in the plane of the waveguide. This latter technique allows to have more freedom in the way the alignment between the fiber must be aligned to the waveguide though the fiber must be normal to the plane of the focusing gratings.

The edge coupling technique is chosen for the neural probes because it reduces the foot-print of the device.

B) Fabrication process

This part describes the process flow to develop the neural probes.

1) Alignment marks development

The first step of the process is to create the alignment marks used for the alignment of the electron-beam lithography of the optical and electrical components. The steps are:

- 1) Spin-coating of a high-contrast and positive photoresist for the electron-beam lithography (ZEP520A);
- 2) Electron-beam lithography to define the alignment marks;
- 3) Development of the positive photoresist using sonication (the baker containing the developing solution and the wafer is put in a batch with water where ultrasounds are used to create waves): this technique allows for removing the exposed areas. Another step is used to make sure the residuals are all gone: an oxygen plasma created thanks to the Reactive Ion Etching (RIE) for 20 seconds (**cf. the exact recipe below**);
- 4) An evaporation of Titanium (10 nm) and Gold (100 nm) is done in the electron-beam evaporator on top of the photoresist in order to define the interconnections, the pads;
- 5) A lift-off process is then made to remove the photoresist which was not exposed during the electron-beam lithography: this helps to keep only the required electrodes and wirings. To do the lift-off process, N –

methyl pyrrolidinone is used at 80°C and the wafer is soaked for one hour and then removed from the batch. To get rid off the Gold particles, acetone and iso-propyl alcohol are sprayed on the wafer.

The recipe to remove the residuals of the photoresist is: RF power = 50 W, Pressure = 30 mTorr, Temperature = 20°C, O₂ = 100 sccm. This step lasts for 30 seconds.

2) Process for the optical part: waveguides, ring resonators and gratings development

Starting from the Lionix TriPleX wafer with the alignment marks, the following steps are followed to develop the waveguides, the ring resonators and the gratings:

- 6) Spin-coating of a photoresist for the electron-beam lithography (ZEP520A);
- 7) Electron-beam lithography to define the waveguides, the ring resonators and the gratings;
- 8) Development of the photoresist in a solution of amyl-acetate to remove the exposed areas. Another step is used to make sure the residuals are all gone: an oxygen plasma created thanks to the RIE for 30 seconds;
- 9) RIE of Si₃N₄ (**cf. the exact recipe below**);
- 10) ZEP520A is then removed by sonication for 10 minutes in dichloromethane and 10 minutes in acetone;
- 11) Plasma-Enhanced Chemical Vapor Deposition (PECVD) of 2.5 µm of SiO₂ for creating the insulation layer between the optical and the electrical layers (**cf. the exact recipe below**);

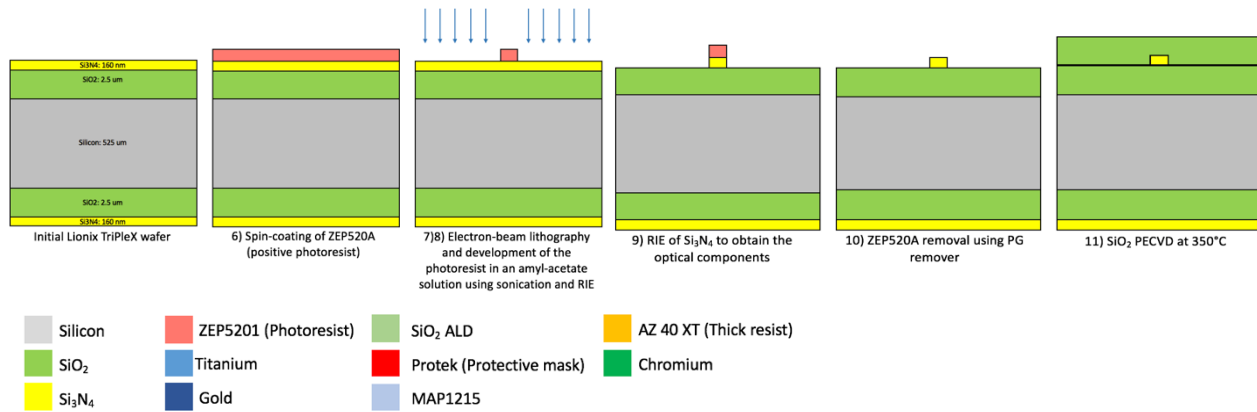


FIG.48: FABRICATION OF THE OPTICAL LEVEL OF THE NEURAL PROBES

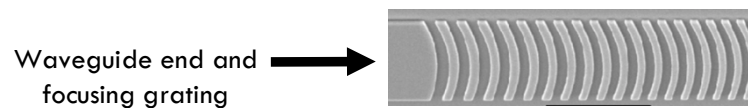


FIG.47: SEM IMAGE OF THE END OF THE WAVEGUIDE AND OF THE FOCUSING GRATINGS

The recipe used to etch the Si₃N₄ with the RIE is: RF power = 51 W, Pressure = 55 mTorr, Temperature = 20°C, CHF₃ = 48 sccm, O₂ = 2 sccm. The etching lasts for 7 min 30 sec. Then, another etching step is done with the following parameters: **RF power = 101 W**, Pressure = 55 mTorr, Temperature = 20°C, CHF₃ = 48 sccm, O₂ = 2 sccm. This etching step lasts for 1 min 30 sec.

The recipe used to deposit SiO₂ with the PECVD at 350°C is: RF power = 20 W, Pressure = 1000 sccm, Temperature = 350°C, Silane/Argon = 1182 sccm, N₂O = 710 sccm. The deposition lasts for 38 min.

3) Process for the electrical part: electrodes, wires and pads development

On top of the Silicon Dioxide layer deposited previously, the following steps are done to create the electrodes to record the neural signals and the wires to connect these electrodes to the pads of the bonding area:

- 12) Spin-coating of a photoresist for the electron-beam lithography (ZEP520A);
- 13) Electron-beam lithography to define the electrodes and the wires;
- 14) Development of the positive photoresist using sonication. Another step is used to make sure the residuals are all gone: an oxygen plasma created thanks to the RIE for 30 seconds (**cf. the exact recipe below**);
- 15) An evaporation of Titanium (10 nm) and Gold (100 nm) is done in the electron-beam evaporator on top of the photoresist in order to define the interconnections, the pads;

- 16) A lift-off process is then made to remove the photoresist which was not exposed during the electron-beam lithography: this allows to keep only the required electrodes and wirings. To do the lift-off process, N – methyl pyrrolidinone is used at 80°C and the wafer is soaked for one hour and then removed from the batch. To get rid off the Gold particles, acetone and iso-propyl alcohol are sprayed on the wafer;
- 17) An Atomic Layer Deposition on top of the electrodes is realized to prevent the neural cells of the brain from getting in contact with the wires using 75 nm of SiO₂;
- 18) Spin-coating of photoresist for the opening of electrodes (the same resist as the one for the optical part is used, cf. III)B)2);
- 19) Electron-beam lithography of ZEP520A and development (the same solution and the same technique as the ones for the optical part are used, cf. III)B)2);
- 20) Opening of the electrodes using RIE etching to etch the SiO₂ using CHF₄ as reactant in the chamber (to avoid misalignment problems, the opening of the ZEP520A is actually smaller than the real gold pad size) (cf. the exact recipe below);
- 21) ZEP520A is then removed by soaking the wafer for one hour in a hot PG remover (80°C) and then acetone and isopropanol are sprayed onto the wafer.

The recipe to remove the residuals of the photoresist is: RF power = 50 W, Pressure = 30 mTorr, Temperature = 20°C, O₂ = 100 sccm. This step lasts for 30 seconds.

The recipe to etch the SiO₂ to open the pads with the RIE is: RF power = 200 W, Pressure = 55 mTorr, Temperature = 20°C, CHF₃ = 35, Ar = 25. This step lasts for 2 min 30 sec.

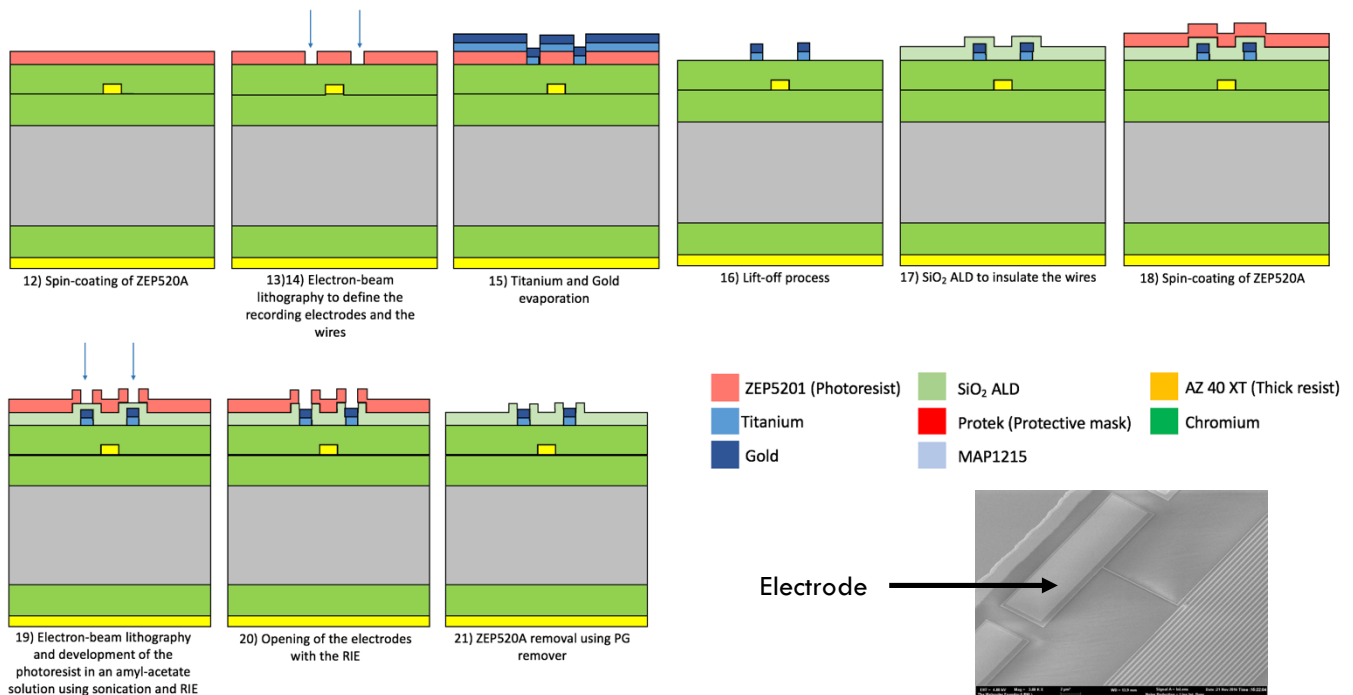


FIG.50: FABRICATION OF THE ELECTRICAL LEVEL OF THE NEURAL PROBES

FIG.50: SEM IMAGE OF THE ELECTRODES INTEGRATED ON THE SHANK OF THE PROBE

4) Releasing the probes

After fabricating the different components for manipulating the neurons and recording the neural signals inside the cortex of the brain, the probes must be released from the wafer: this is done in two different steps.

a) Back-side etching

A back-side etching of the wafer is first done. As a reminder, at the back of the wafer, there are two layers to etch before reaching the Silicon: 160 nm of Si₃N₄ and 2.5 µm of SiO₂. These layers are etched using dry etching techniques.

To etch the Silicon substrate and so to define the thickness of the neural probe, a protective layer is spun on the front side of the wafer before starting the KOH etching: this mask is called Protek®. This mask is used in order to protect the electrical components integrated on the front-side of the wafer that could be etched during the KOH etching.

The following steps are followed for the back-side etching:

- 22) Spin-coating of MAP1215 to protect the front-side of the wafer while etching Si_3N_4 and SiO_2 because the wafer is flipped during these steps (**cf. the exact recipe below**);
- 23) Evaporation of a hard mask made of Chromium at the electron-beam evaporator on the back-side of the wafer (300 nm);
- 24) 5 minutes of UV ozone cleaning;
- 25) Spin-coating of a layer of HDMS on the back-side of the wafer to ease the adhesion of the photoresist and spin-coating of MAP1215, the photoresist;
- 26) A mask is aligned to the alignment marks and this mask is put in contact with the wafer. The wafer is exposed at the UV light for 5 seconds and developed for 60 seconds in a basic solution (MAD331 – Sodium Hydroxide);
- 27) Chromium etching using Chromium etchant;
- 28) RIE is used to etch Si_3N_4 (**cf. the exact recipe below**);
- 29) Capacitively-Coupled Plasma (CCP) is used to etch SiO_2 (**cf. the exact recipe below**);
- 30) MAP1215 is removed by putting the wafer in an acetone baker for 10 min, then by spraying iso-propyl alcohol on the wafer, then by putting the wafer in an iso-propyl alcohol baker for 2 min, then by spraying iso-propyl alcohol in the wafer, and finally using nitrogen gas to remove the dust;
- 31) Chromium is removed with Chromium etchant for 15 min (the wafer must be put softly in the bake in order not to break it);
- 32) Spin-coating of Protek® (**cf. the exact recipe below**);
- 33) A KOH solution (33%) heated up to 85°C and stirred is used to etch the Silicon up to $50\ \mu\text{m}$. It is difficult to stop at this thickness because the initial thickness of the Silicon layer may vary from one wafer to another according to the accuracy in the fabrication process of the Lionix TriPleX wafer;
- 34) Protek® removal with Protek remover and then Iso-propyl alcohol for 3 min.

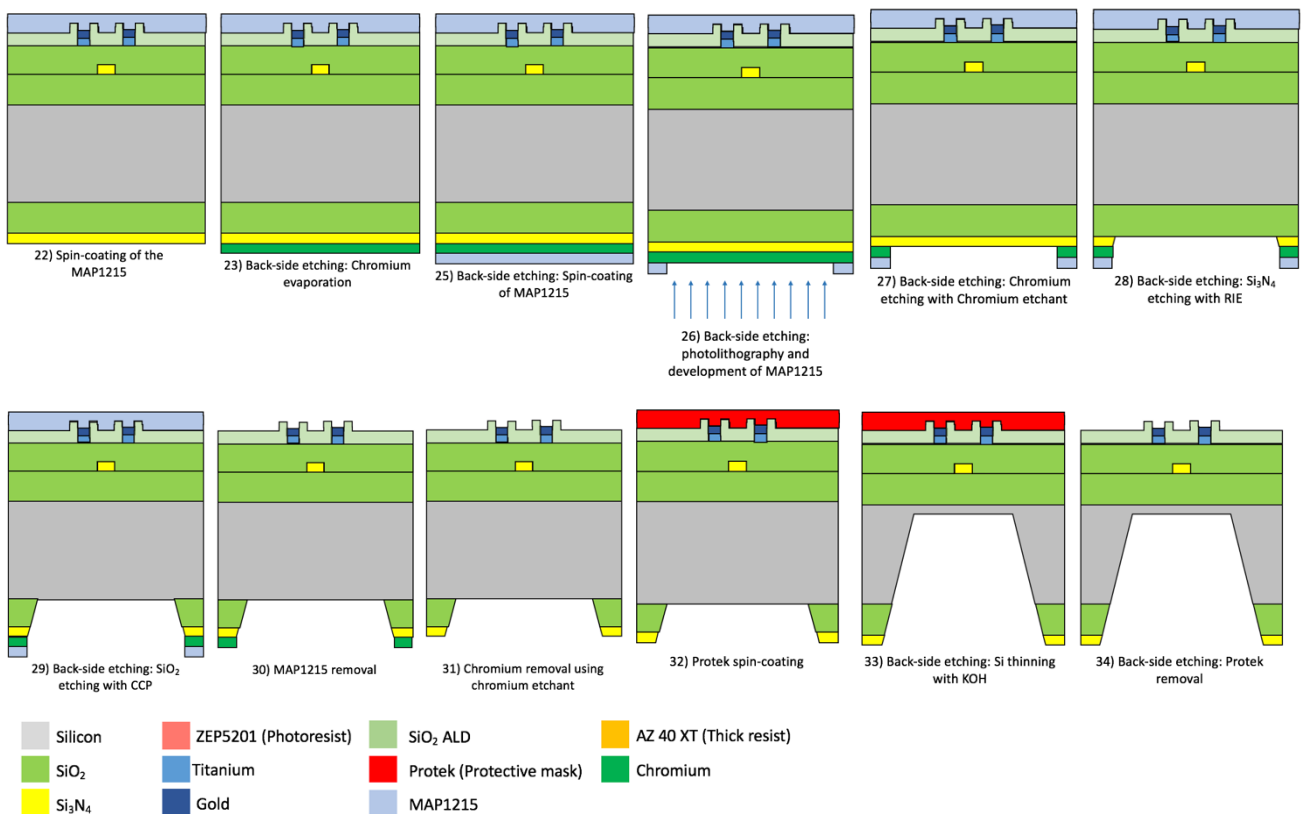


FIG.51: BACK-SIDE ETCHING OF THE NEURAL PROBES TO DEFINE THEIR FINAL THICKNESS

The recipe to spin-coat the Protek® is:

- Spin-coating of the primer (adhesion layer): 1500 rpm, 1000 rpm/s, 60 s
- Bake on hot-plate at 205°C for 60 sec
- Nitrogen gas on the wafer to remove the dust
- Spin-coating of the first layer of Protek®: 1000 rpm, 5000 rpm/s, 60 s
- Bake on hot-plate at 110°C for 2 min
- Spin-coating of the second layer of Protek®: 1000 rpm, 5000 rpm/s, 60 s
- Bake at 110°C for 2 min
- Bake at 205°C for 1 min

The final thickness of Protek® is on the order of 17 μm to 19 μm .

The recipe used to etch the Si_3N_4 with the RIE is: RF power = 51 W, Pressure = 55 mTorr, Temperature = 20°C, CHF_3 = 48 sccm, O_2 = 2 sccm. The etching lasts for 7 min 30 sec. Then, another etching step is done with the following parameters: **RF power = 101 W**, Pressure = 55 mTorr, Temperature = 20°C, CHF_3 = 48 sccm, O_2 = 2 sccm. This etching step lasts for 1 min 30 sec.

During the KOH etching, it is important to remove the wafer often from the batch and to check the remaining thickness of the Silicon layer to make sure the etching rate is not too fast and not too much Silicon is etched.

b) Front-side etching

The final step to release the probes from the wafer is the front side etching of the wafer. Several layers must be etched: 2.5 μm of SiO_2 , 75 nm of SiO_2 deposited with the ALD, 160 nm of Si_3N_4 , 2.5 μm of SiO_2 , the remaining thickness of Silicon after the KOH etching.

The etching of the layers must produce sidewalls as straight as possible. Indeed, once the probe is released, the waveguide integrated on the shank is coupled to an optical fiber in order to shine light inside the brain and, in order to limit the losses at the interface between the two components and to ease the alignment, the surface of the probe must be as flat as possible. Also, the undercut must be limited in order to have a thickness of Silicon high enough to insert the probe inside the cortex without breaking them.

A protective layer must be used in order to protect all the parts of the wafer that should not be etched. A thick resist called AZ-40XT-11D is used.

- 35) Spin-coating of the thick resist AZ-40XT-11D (cf. the exact recipe below);
- 36) Exposure of AZ-40XT-11D for 12.5 sec at a power density of 14.5 mW/cm² at the UV-photolithography and development using the resist developer MF26A for 4 min 30 sec (to create a width of approximately 100 μm) (cf. the exact recipe below);
- 37) CCP etching of SiO_2 (75 nm + 2.5 μm PECVD), of Si_3N_4 (160 nm) – not represented for simplification, of SiO_2 (2.5 μm LPCVD) (cf. the exact recipes below);
- 38) Inductively-Coupled Plasma etching of the Silicon (cf. the exact recipe below);
- 39) Thick resist removal with AZ 400 T for 30 minutes at 77.5°C.

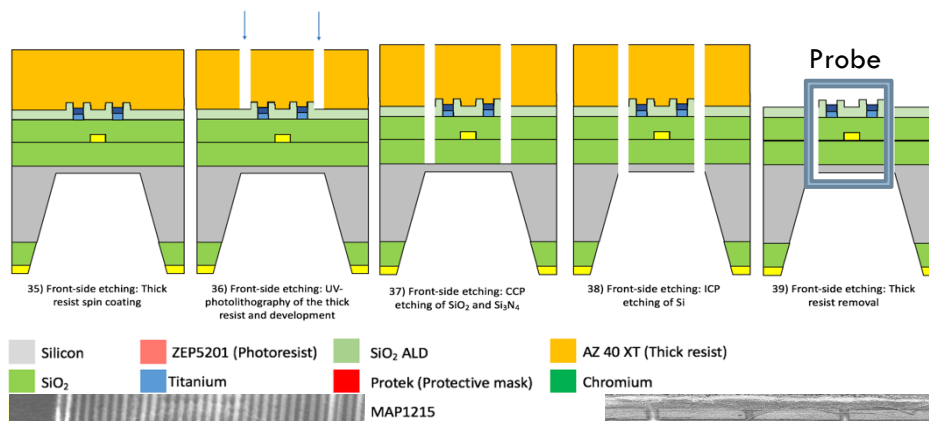
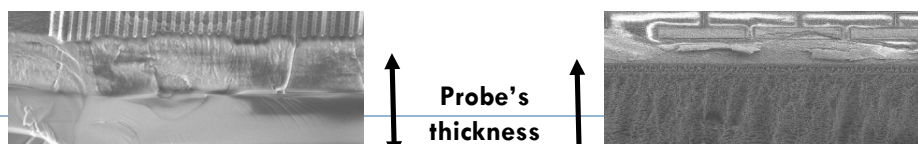


FIG.52: FRONT-SIDE ETCHING OF THE NEURAL PROBES TO RELEASE THEM



The recipes used to spin-coat the thick resist and to expose it are:

- 5 min UV ozone
- Spin-coating of the adhesive layer HMDS: 2000 rpm, 1000 rpm/s, 45 s
- Bake on hot plate with Silicon pieces between the wafer and the plate: 100°C for 5 min
- Spin-coating of AZ-40XT-11D: 1750 rpm, 5000 rpm/s, 20 s
- Soft-bake: 60°C for 20 min, 80°C for 20 min, 100°C for 10 min, 125°C for 10 min, then let the wafer cool down to room temperature
- Exposure of the wafer edges for 12.5 seconds at 14.5 mW/cm²
- Post-Exposure Bake: 60°C for 1 min, 80°C for 1 min, 95°C for 1 min, 115°C for 1 min, then let the wafer cool down to room temperature
- Development for 8 min in MF26A
- Exposure of the whole wafer for 12.5 seconds at 14.5 mW/cm²
- Post-Exposure Bake: 60°C for 1 min, 80°C for 1 min, 95°C for 1 min, 115°C for 1 min, then let the wafer cool down to room temperature
- Development for 4 min 30 sec in MF26A

To etch the SiO₂ and Si₃N₄ layers, the CCP is used with the following recipe: RF power = 150 W, VHF power = 400 W, Pressure = 20 mTorr, Temperature = 20°C, CF₄ = 35 sccm, Ar = 15 sccm, O₂ = 10 sccm. The etching lasts for approximately 1 hour. It is important to keep the temperature of the wafer at 20°C otherwise it may burn.

To etch the remaining thickness of Silicon, ICP is used: RF power = 20 W, ICP power = 700 W, Pressure = 6 mTorr, Temperature = 20°C, SF₆ = 26 sccm, O₂ = 24 sccm. The etching lasts for approximately 1 hour 30 min.

5) Electrodes electroplating

After the probes are released, they are glued on a PCB using Epoxy glue. Then, the probes are wire-bonded to connect the pads of the bonding area to the connections of the PCB used to interface with the external world. The **Fig.54** and **Fig.55** show these two steps.

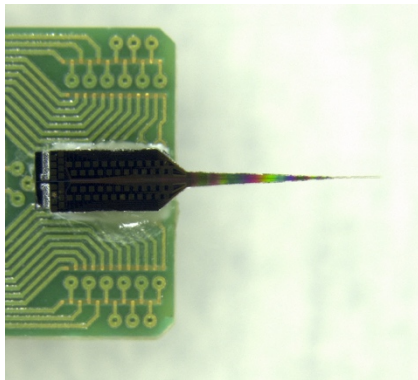


FIG.55: MICROSCOPE IMAGE OF THE NEURAL PROBE GLUED ON THE PCB USING EPOXY GLUE

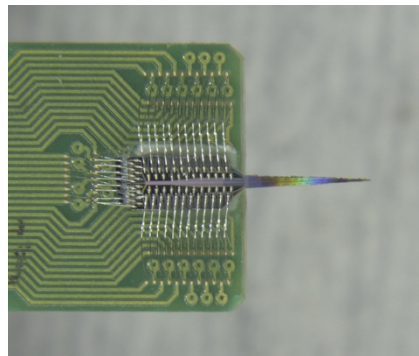


FIG.54: MICROSCOPE IMAGE OF THE NEURAL PROBE GLUED ON THE PCB AND WIRE-BONDED

The last step required is an electroplating of the electrodes integrated on the shank of the probe.

To be able to sense the neural signals generated by the neurons, on the order of a few μV , the impedance of the electrodes must be low, below $1\text{ M}\Omega$ [63]. However, due to the small dimensions of the electrodes integrated on the probes, their impedance is high, limiting the signal-to-noise ratio [43]. One of the available solution to reduce the electrodes' impedance is to use electroplating i.e. depositing another material on top of the electrodes, like Platinum or Gold, in order to reduce the electrode impedance by increasing the surface area and roughness of the electrodes.

A solution of Black Platinum is used for the electroplating of the neural probes. The probe and a reference electrode are put in the solution of Black Platinum and a NanoZ apparatus is used to apply a DC current of $-0.1\mu\text{A}$ for 12 sec between the probe's electrodes and a reference electrode: tens of nm of Platinum are deposited on top of the gold electrodes. It was determined that an impedance below $1\text{ M}\Omega$ is required to read well action potentials [63]. Before electroplating, the impedance was measured to be $4.5 \pm 0.1\text{ M}\Omega$ at 1000 Hz and after electroplating, the impedance becomes $200 \pm 30\text{ k}\Omega$ at 1000 Hz [63]: reducing the impedance by a factor of 20 should allow to read better the APs.

C) Budget

The tools used in the laboratories are at the state-of-the art. Developing a neural probe is resource-consuming and a careful optimization of the parameters is required to have a high yield for the electrodes as well as a high optical components efficiency. However, considerable research effort is required to cure neurodegenerative disorders because it is affecting 0.5% of the world's population for what concerns Alzheimer [70]. In this part, a brief review of the cost of the raw material as well as of the tools used to process the wafer is given.

The Lionix TriPleX wafer is the raw material for the probes. Its cost is \$500: it is a very expensive wafer when compared to a classic silicon wafer whose price is on the order of tens of dollars. A Silicon wafer could be used and LPCVD could allow to deposit the layers required for the optical components at a lower cost, however, an optimization of the parameters would need to be done.

One wafer allows to release approximately 100 probes. The unit cost for an order of 100 PCBs on which the probes are glued is \$25. Also, two connectors are required per PCB to interface with the electronics treatments tools, they cost \$10 each. Then, the production cost for one probe is on the order of \$50. To this price, the cost of the fiber used to bring light inside the brain must be added.

For what concerns the tools used, the prices are given below:

Tools: ALD: approximately 1.5 million €; Electron-beam lithography: approximately 4 million €; PECVD: approximately 150k€; RIE: approximately 150k€; SEM: approximately 1 million €; CCP/ICP: approximately 300k€ each.

For what concerns the optical tools used to test the neural probes, the prices are given below:

Optical set-up: Linear stages: 2k€; Micro-manipulators: 3k€; CCD camera: 200€; Fiber splicer: 10k€; Fiber cleaver: 1k€; Optical fiber used to connect the laser and the waveguide of the probe: 10€ for 1 meter; Patch-cord to connect the fiber at the output of the laser and the fiber used to interface the waveguide: 100€ for 1 meter; Laser used to test the probes: 3k€; Microscope used to observe the gratings: 4k€.

Must also be considered the cleanroom functioning costs, the other tools and the chemicals available.

IV) RESULTS AND DISCUSSION

During the internship, optoelectronic probes have been released. In this part, the results that have been obtained as well as the choices that have been made to try to improve the optical efficiency of the probes are explained.

A) Fabrication of optoelectronic probes

Following the steps III)B)1)2)3)4), optoelectronic probes have been released from the Lionix TriPleX wafer. Some pictures of the probes fabricated are shown below.

First, Silicon probes have been released, as seen on the Fig.56.

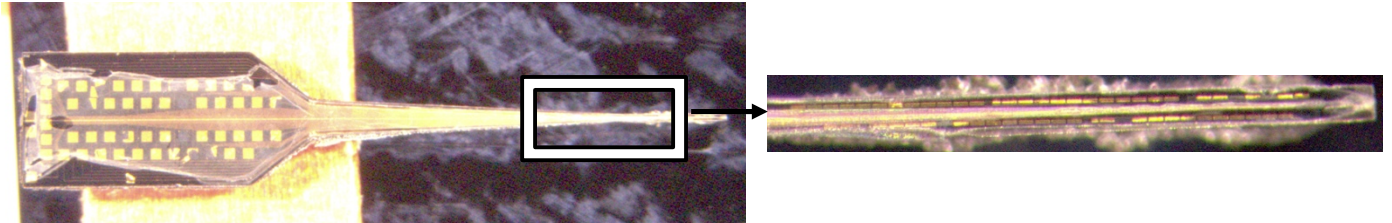


FIG.56: SILICON NEURAL PROBE WITH A FOCUS ON THE SHANK ON THE RIGHT PICTURE

Then, using an undercut process, Silicon Dioxide probe have been obtained, as seen on Fig.57.

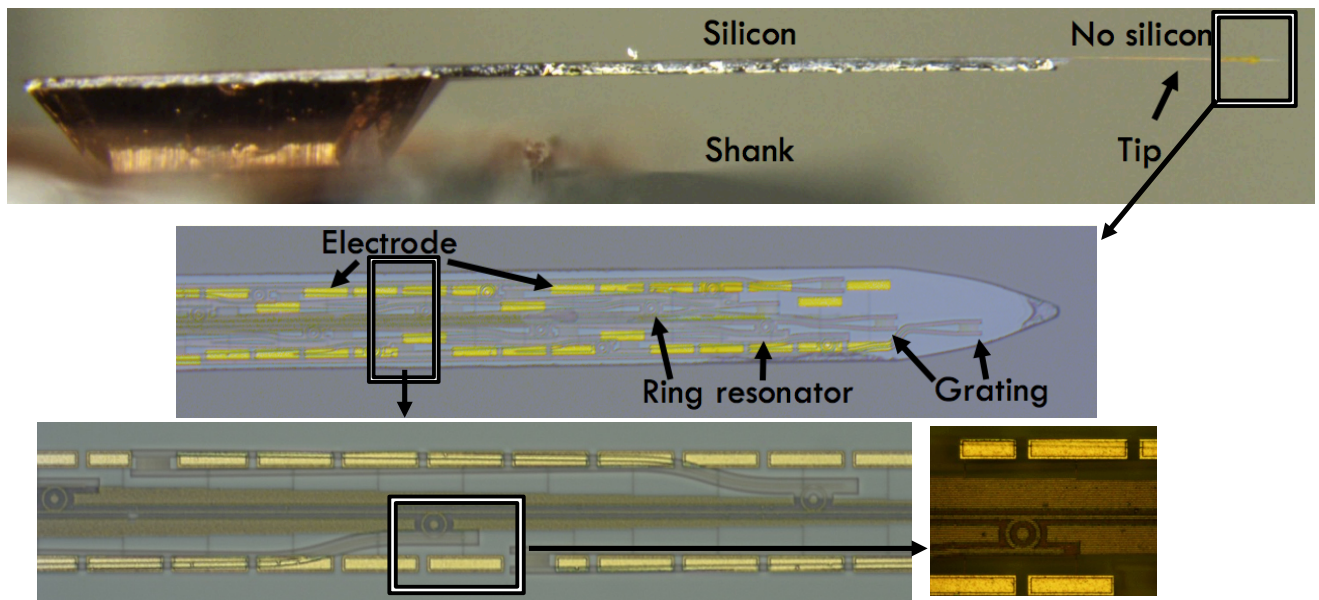


FIG.57: OXIDE NEURAL PROBE

The probe presented above has a shank which is 900 μm long, 50 μm wide and 5.2 μm thick. Due to an isotropic etching, the substrate has been removed from below the shank. This is why the shank obtained is transparent: there is only a layer of Silicon Dioxide remaining (and the layers for the components integrated on the probe). The electrodes, waveguides, ring resonators and gratings can be observed on the last pictures.

B) Tests of the optical components integrated on the probes

After releasing the probes, they must be tested. The focus was first made on the optical components.

1) Fiber gluing

As explained before, in order to bring light in the central waveguide integrated on the shank of the neural probe, a tunable-wavelength laser is connected to an optical fiber which is then coupled to the waveguide and finally, this fiber is glued on the probe.

The laser used is single-mode and lasing at 450 nm. The wavelength of the laser can be tuned in the range of 448.6 nm to 452.7 nm.

The fiber core is 4 μm in diameter and the cladding around the core is 125 μm . Before the alignment between the optical fiber and the waveguide, the fiber protective coating must be stripped away and the tip of the fiber cleaved to make sure the light spot is circularly uniform (cleared from any particle or defect).

This fiber is then aligned to the waveguide using a set-up that can be seen on the [Fig.58](#).

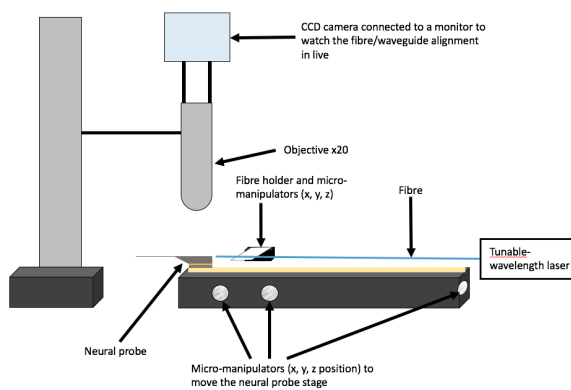


FIG.59: OPTICAL SET-UP TO OBSERVE THE OPTICAL COMPONENTS AND TO GLUE THE FIBER ON THE NEURAL PROBE

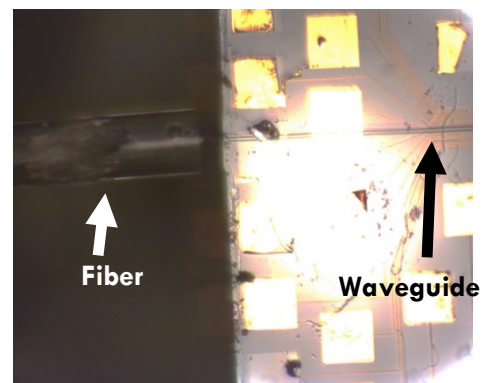


FIG.58: THE FIBER IS APPROACHED CLOSE TO THE WAVEGUIDE TO DO THE ALIGNMENT AND THE FIBER GLUING

Micro-controllers are used in order to precisely align the waveguide and the fiber: a good alignment means there is a high coupling efficiency between the fiber and the waveguide. The alignment parameters are: the gap between the fiber and the waveguide, the tilting of the fiber with respect to the waveguide, the misalignment in the x and y directions.

Then, a microscope and a CCD camera are used to observe the alignment between the waveguide and the fiber at the entrance of the waveguide; then, to make sure the alignment is good, the camera is placed over the tip's output grating to see whether they are radiating light or not: when light can be observed at the tip, the intensity is increased by optimizing the alignment with the micro-controllers. To make sure the light observed at the tip is not due to scattering of the fiber light on the probe, the wavelength of the laser is tuned: if different ring resonators are radiating light for different wavelength, there is no scattering.

After the alignment, the fiber must be glued on the probe in order to allow the insertion of the probe inside the brain: it would not be convenient to align the fiber and the waveguide directly inside the brain for practical reasons. To glue the fiber on the probe, a UV-curable glue, called OP6725® is deposited on the tip of the fiber.

After the glue is present on the fiber's tip, the fiber is aligned again with the waveguide using a red-light laser to make sure the glue is not going to get cured. Once the alignment is obtained, the red-laser is switched off and the UV-laser (405 nm wavelength) switched on to cure the glue for 15 seconds. The two lasers (red and blue) are connected to a 50-50 splitter allowing to switch them on and off alternatively, without having to change the fiber, which is important not to lose the alignment fiber / waveguide. After the glue is cured, a blue-laser is used to make sure the alignment has not been lost during the gluing.

On the figure [Fig.59](#), the mechanical stability of the fiber once glued to the waveguide is not high enough to allow the fiber to remain attached when the neural probe is removed from the set-up. In order to improve the mechanical contact between the fiber and the waveguide, a probe with a new design was developed: this new design integrates a V-groove on the bonding area, i.e. a trench where the fiber can be inserted and for which the gluing should be more easy.

The V-groove is 140 μm wide and 1.2 mm long. The cladding of the fiber is 125 μm in diameter, so the V-groove is 15 μm wider to account for the possible misalignment of the V-groove during the optical lithography. The sketch **Fig.60** explains how the fiber is inserted in the V-groove of the probe.

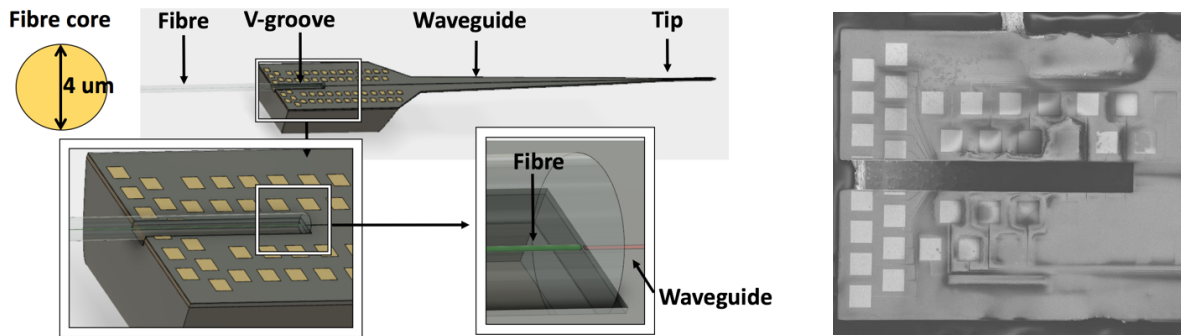


FIG.60: SKETCH AND SEM IMAGE OF THE V-GROOVE ETCHED ON THE NEURAL PROBE TO EASE THE FIBER GLUING

2) Test of the ring resonators

First, the functioning of the ring resonators has been tested. To do so, the wavelength of the laser was tuned to check if different ring resonators were coupling the light for different wavelengths.

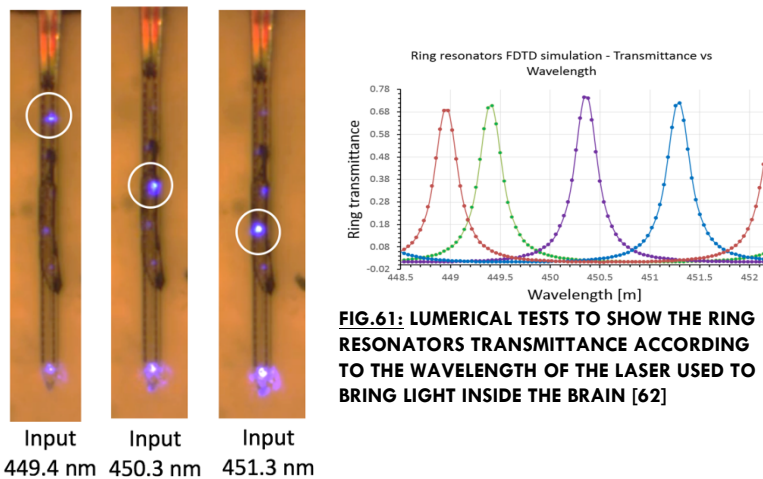


FIG.61: LUMERICAL TESTS TO SHOW THE RING RESONATORS TRANSMITTANCE ACCORDING TO THE WAVELENGTH OF THE LASER USED TO BRING LIGHT INSIDE THE BRAIN [62]

FIG.62: DIFFERENT RING RESONATORS ARE SHINING FOR DIFFERENT WAVELENGTHS

As it can be seen on the **Fig.61**, for different input wavelengths, different luminous spots are shining on the shank of the probe and so different ring resonators are trapping the light coming from the central waveguide: this proves the functioning of the ring resonators and this is coherent with the simulations that had been done with Lumerical®.

The coupling efficiency, corresponding to the amount of light trapped by one ring resonator with respect to the amount of light that is trapped by all the rings on the same shank has been determined, for their specific resonance wavelength. To compute the coupling efficiency, the power radiated by one grating of the shank was divided by the sum of the powers radiated by all the gratings of the shank.

Wavelength optimized for 1st ring		Wavelength optimized for 3rd ring		Wavelength optimized for 5th ring	
Ring #	Ring coupling efficiency percentage	Ring #	Ring coupling efficiency percentage	Ring #	Ring coupling efficiency percentage
1	52,22	1	0,00	1	23,51
2	0,00	2	0,00	2	13,52
3	0,00	3	79,15	3	0,00
4	6,23	4	0,00	4	4,45
5	7,24	5	0,00	5	28,15
Tip	34,31	Tip	20,85	Tip	30,37
Wavelength optimized for 2nd ring		Wavelength optimized for 4th ring		Average coupling efficiency	
Ring #	Ring coupling efficiency percentage	Ring #	Ring coupling efficiency percentage	64	
1	0,00	1	0,00		
2	78,03	2	0,00		
3	0,00	3	4,01		
4	16,15	4	81,22		
5	0,00	5	0,00		
Tip	3,41	Tip	14,77		

TABLE 1: COUPLING EFFICIENCY FOR THE DIFFERENT RING RESONATORS INTEGRATED ON THE SHANK OF THE NEURAL PROBE

The average coupling efficiency for the rings has been determined to be 64%. The coupling efficiency of the rings depends on parameters such as the gap between the central waveguide and the ring's centers and the nano-fabrication related defects in the ring itself. If a high coupling efficiency is reached from the measurements done previously, it is because the spectral width of the laser used for a specific wavelength is larger than the one that was computed in the simulations, leading to an increase of the coupling efficiency because more light can be coupled inside the ring. Indeed, as shown on the left graph [Fig.63](#) where the relative transmittance was experimentally measured for each ring resonator, the spectral width is on the order of 0.5 nm whereas it is on the order of 0.25 nm on the Lumerical® simulations of the right graph [Fig.64](#), where the spectral width of the laser is also shown.

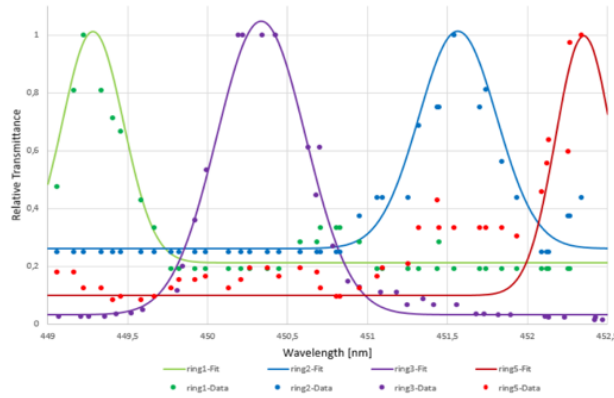


FIG.64: EXPERIMENTAL TRANSMITTANCE OF THE RING RESONATORS [62]

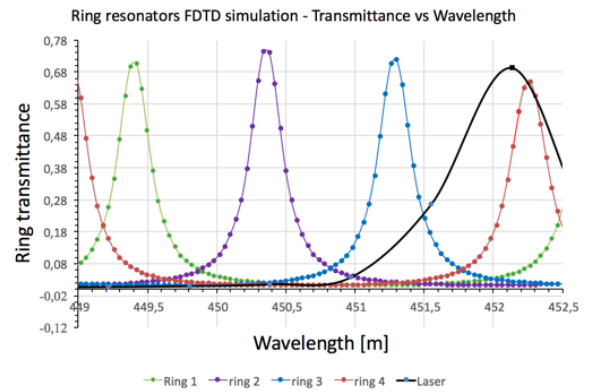
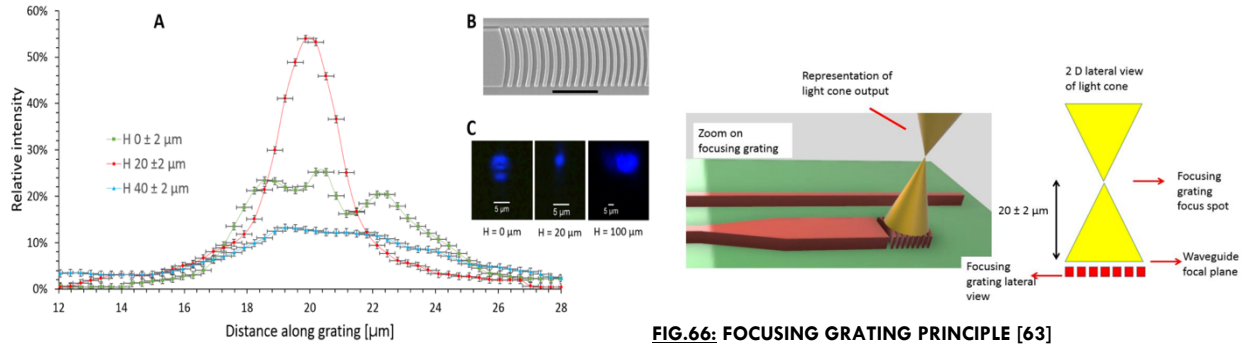


FIG.63: LUMERICAL SIMULATION OF THE RING RESONATORS TRANSMITTANCE [62]

These results demonstrate that ring resonators can be used to passively switch light on different areas of the neural probes.

3) Test of the focusing gratings

Focusing gratings can be used to focus a specific wavelength at a certain height above the plane of the probe. The gratings designed for the neural probes allow to focus blue light (450 nm) at a height of 20 μm within a 1 μm diameter spot. If other wavelengths are used, the luminous spot will have more aberrations and the focusing height and angle may be different. Here, the gratings developed on the probes are tested by taking pictures of the spot at different heights above the probe's plane and by plotting the profile of the spot for the different pictures. The result is shown [Fig.65](#).



From the [Fig.65](#), it can be seen that at the heights 0 μm and 40 μm , the luminous spot is wider than it is at 20 μm , which should be the height of the central spot, which is coherent with the way focusing gratings must be working. Also, the peak intensities for 0 μm and 40 μm are lower than the one for 20 μm . This result shows that focusing grating can be used to reach areas of the brain 20 μm away from the probe's shank and to focus light within a very small spot to reach specific neurons.

4) Power measurements from the probes and sources of losses

a) Power extracted from the focusing gratings

When the alignment is done and the fiber glued to the waveguide, the power radiated by the gratings can be computed. From the pictures taken switching the different gratings, it is possible to extract the power radiated by the spot using the software ImageJ after the power at the output of the fiber was used as a reference. On the [Fig.67](#), some of the pictures taken for different wavelengths. The way the power was computed is described in the [Appendix 2](#).

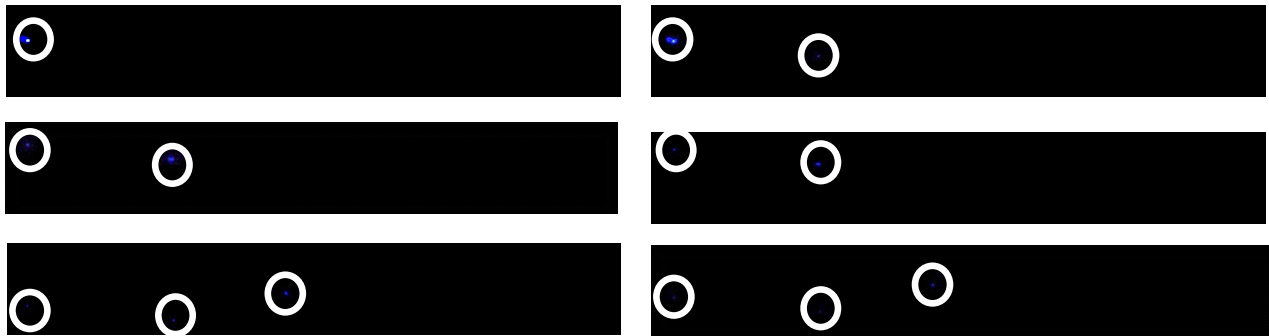


FIG.67: DIFFERENT RING RESONATORS ARE SHINING FOR DIFFERENT WAVELENGTHS. WAVELENGTHS FROM LEFT TO RIGHT AND TOP TO BOTTOM: 449.22 NM, 449.80 NM, 450.30 NM, 450.97 NM, 451.55 NM, 452.13 NM. CCD EXPOSURE TIME = 0.01 MS

The contrast and the luminosity of the pictures above have been increased for representation purposes.

The [Table 2](#) presents the results of the power radiated for the probe without the V-groove.

Exposure time (ms)			Wavelength (nm)		
0,01			449,22		
Ring number	Power density (W/mm2)	Power (W)	Ring number	Power density (W/mm2)	Power (W)
1	6,77E-03	2,71E-08	1	5,31E-03	2,12E-08
2	4,46E-05	1,78E-10	2	1,58E-04	6,33E-10
3	Non visible		3	Non visible	
4	Non visible		4	Non visible	

TABLE 2: POWER EXTRACTED FROM THE GRATINGS FOR THE CLEAVED ENTRANCE NEURAL PROBE

The power density required to activate the genetically-modified neurons ranges between 0.1 mW/mm² [67] and 1.1 mW/mm² [68] using LEDs. From the measurements presented in the table above, the power radiated by the gratings is not high enough to activate the gratings, except for the rings highlighted in green. However, because the focusing gratings radiate coherent light and because they are located close to the neurons, the power required to activate the opsins may be lower than the one given in the two previous papers.

The polarization of the light has an influence on the power radiated by the gratings. Indeed, the waveguide simulations and the waveguide design have been made considering the mode TE₀ (Transverse Electric), for which the electrical field is maximal at the center of the waveguide and decreases towards the boundary. To take into account this parameter, for the probe with the V-groove, the polarization of the light is controlled using a polarization-controller developed by Thorlabs® which allows to tilt the fiber modifying the polarization. So in the **Table 3**, the wavelength of the laser was optimized for each ring, and there is a minimum and a maximum for both the power density and the power: they correspond to the light polarization leading to the lowest results and to the light polarization leading to the highest result.

Wavelength optimized for the 1st ring					
Ring #	Min power (W)	Min power density (W/mm ²)	Max power (W)	Max power density (W/mm ²)	Polarization influence in percentage
1	9,27E-10	4,12E-04	2,55E-09	1,14E-03	64
2	4,15E-10	1,85E-04	0,00E+00	0,00E+00	0
3	6,24E-10	2,77E-04	9,67E-10	4,30E-04	35
4	2,89E-10	1,28E-04	5,97E-10	2,65E-04	52
5	8,13E-10	3,61E-04	8,52E-10	3,79E-04	5
Tip	4,19E-10	1,86E-04	1,19E-09	5,30E-04	65
Wavelength optimized for the 3rd ring					
Ring #	Min power (W)	Min power density (W/mm ²)	Max power (W)	Max power density (W/mm ²)	Polarization influence in percentage
1	1,04E-09	4,64E-04	3,51E-09	1,56E-03	70
2	3,09E-10	1,37E-04	4,08E-10	1,81E-04	24
3	7,64E-10	3,40E-04	1,33E-09	5,91E-04	42
4	3,54E-10	1,57E-04	1,12E-09	4,97E-04	68
5	2,91E-10	1,29E-04	4,29E-10	1,90E-04	32
Tip	1,05E-09	4,67E-04	1,73E-09	7,69E-04	39

TABLE 3: POWER EXTRACTED FROM THE GRATINGS FOR THE V-GROOVE NEURAL PROBE

In the previous table, the last column, called “Polarization influence in percentage”, determines the percentage difference between the maximum and the minimum powers.

From the previous tables, the power radiated by the gratings would allow to activate the opsins once the probes are inserted in the brain.

The power radiated by the focusing gratings on the two design of probes that have been tested (cleaved input and V-groove) is similar. However, the V-groove probe allows to reach a higher stability of the optical fiber once it is glued on the probe.

Because the brain tissue is very scattering, the light radiated inside the brain to reach the neurons may be absorbed before reaching the opsins [71]. When the gratings are tested before the insertion of the neural probe inside the brain like done previously, a higher threshold of activation must be considered to take into account this scattering effect inside the brain.

b) The losses of the optical circuit limit the power radiated by the focusing gratings

In order to increase the power radiated at the output of the neural probes, the losses in the whole circuit must be studied. The total losses in the circuit have been determined taking the logarithm of the ratio between the total power radiated by the grating of one neural probe and the power radiated at the output of the optical fiber. These losses are on the order of 55 dB.

The main source of losses is the low coupling efficiency between the fiber’s core and the waveguide. Indeed, these losses have been estimated to be 40 dB.

Then, some losses are introduced in the optical circuit:

- Because of the roughness of the sidewalls of the waveguide, losses are induced: these losses have been measured using test structures and are 8.1 dB/cm for blue light (450 nm) and 5.4 dB/cm for red light (650 nm) [66]. Because the length of the waveguide from the bonding area of the neural probe to the shank is on the order of 1 cm, 8 dB are of light intensity are lost due to the waveguide sidewalls; they are on the order of 1 to 2 dB (Silicon photonics);

- Because the ring resonators do not trap all the light from the central waveguide and because they have fabrication defects, losses are introduced: they are on the order of 1 dB to 2 dB;
- Because the focusing gratings do not allow to extract all the light from the waveguide to focus it inside the brain, losses are introduced: they are on the order of 3 dB to 6 dB.

Most of the losses are coming from the low coupling between the optical fiber and the waveguide.

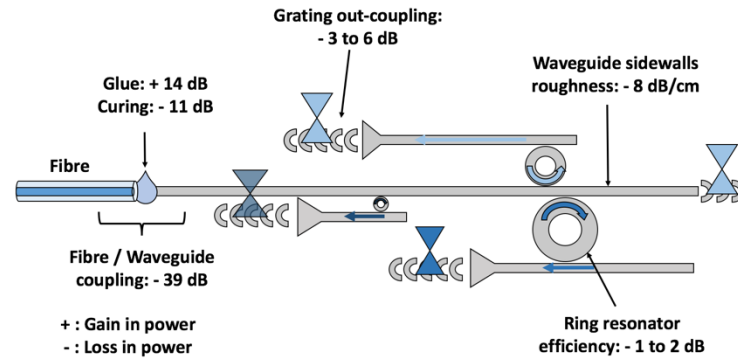


FIG.68: REPRESENTATION OF THE LOSSES OF THE OPTICAL CIRCUIT

One way to improve this coupling efficiency is the glue used to connect the fiber and the waveguide. Indeed, the glue used has a refractive index close to the one of the optical fiber core (1.55 when cured [72]). This glue allows then to increase the coupling efficiency between the fiber and the waveguide because it reduces the angle of dispersion of the light at the output of the fiber, as it can be seen on the [Fig.69](#).

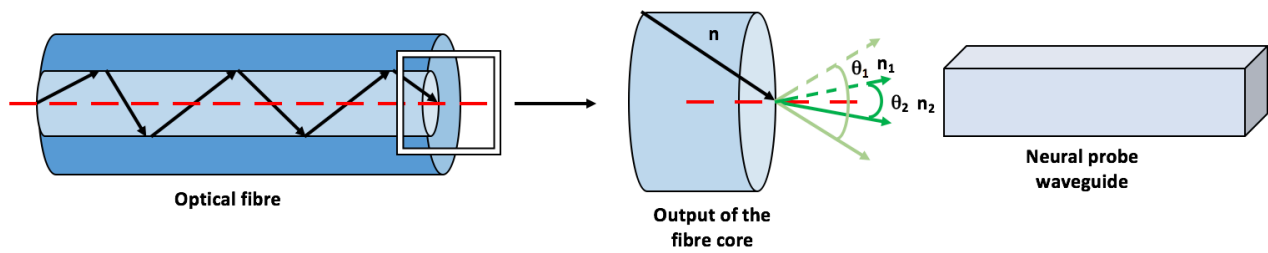


FIG.69: EXPLANATION OF THE VARIATION OF THE ANGLE OF DISPERSION WHEN THE GLUE IS APPLIED AT THE INTERFACE BETWEEN THE FIBER AND THE WAVEGUIDE

At the output of the optical fiber core, there is a change of medium (and so a change in refractive index): the light ray will be refracted at the output of the fiber core according to the Snell's law with respect to the normal of the plane of incidence of the incident light ray. According to this law, the higher the difference in the refractive index of the fiber's core and of the output medium, the higher the refraction angle with respect to the normal; so, if the medium between the optical fiber and the waveguide is air ($n_1 = 1$ and θ_1), the angle of dispersion of the beam at the output of the core will be larger than if the medium between the fiber and the waveguide is glue ($n_2 = 1.55$ when cured and θ_2): this allows the waveguide to collect more light with glue at the interface than with air and so to increase the coupling efficiency.

This result can be observed on the [Fig.70](#) where the light radiated by one focusing grating is observed.

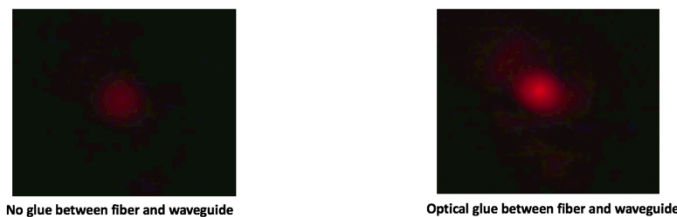


FIG.70: INFLUENCE OF THE GLUE ON THE INTENSITY OF THE FOCUSING GRATING AT THE END OF THE NEURAL PROBE

Using the glue, the light intensity is increased. The increase in intensity has been estimated to be of 14 dB.

However, when the glue is cured, misalignment occurs despite the fact that the glue used is low shrinkage: this leads to a loss in light intensity of approximately 11 dB.

Overall, the probes released demonstrated the functioning of the ring resonators: for different wavelengths, different rings are shining light and couple the light present in the main central waveguide. However, the power radiated by the focusing gratings would probably not allow to activate the opsins, knowing that in the brain, the tissues may absorb visible light decreasing the power reaching the neurons. Ways to improve the coupling efficiency between the fiber and the waveguide must be found to increase the power radiated by the focusing gratings inside the brain because most of the losses are coming from this interface.

c) Improving the coupling efficiency between the optical fiber and the waveguide using a nano-imprinted lensed-fiber

aBeam Technologies, a company working at the Molecular Foundry, is developing nano-imprinted lenses on fiber allowing to focus the light spot coming out of the fiber core. These lenses, whose diameter is on the order of $6\text{ }\mu\text{m}$, have a high refractive index ($n = 1.68$) allowing to focus light in media like the UV-curable glue used to glue the fiber on the waveguide. According to the simulations carried out in [73], whose one result is shown **Fig.71**, the light can be focused within a 730 nm spot for a 660 nm light. Focusing the light using such a lensed-fiber can allow to increase the mode-matching between the optical fiber and the waveguide and so increase the coupling efficiency between both of them.

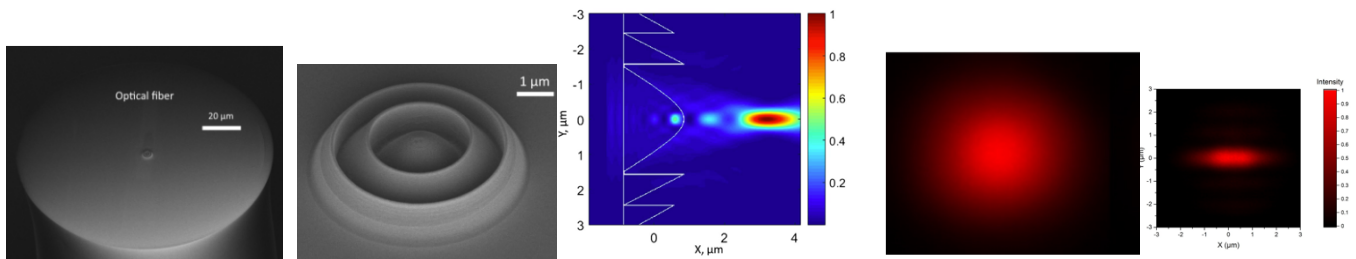


FIG.71: SEM IMAGES OF THE LENS NANO-IMPRINTED ON THE FIBER AND IMAGES SHOWING ITS INFLUENCE ON THE LIGHT AT THE OUTPUT OF THE FIBER
As seen on the two pictures above with the red luminous spot, the lensed-fiber allows to focus the light beam within a very narrow shape.

Using this optical fiber, but without gluing it to the waveguide, the power density radiated by the focusing gratings has been measured and the results are shown in the **Table 4**.

Wavelength optimized for the 1st ring			Wavelength optimized for the 3rd ring			Wavelength optimized for the 5th ring		
Ring #	Power density (W/mm ²)	Power (W)	Ring #	Power density (W/mm ²)	Power (W)	Ring #	Power density (W/mm ²)	Power (W)
1	9,77E-03	2,20E-08	1	0,00E+00	0,00E+00	1	3,02E-03	6,79E-09
2	0,00E+00	0,00E+00	2	0,00E+00	0,00E+00	2	1,74E-03	3,90E-09
3	0,00E+00	0,00E+00	3	2,48E-02	5,59E-08	3	0,00E+00	0,00E+00
4	1,16E-03	2,62E-09	4	0,00E+00	0,00E+00	4	5,71E-04	1,28E-09
5	1,35E-03	3,05E-09	5	0,00E+00	0,00E+00	5	3,61E-03	8,13E-09
Wavelength optimized for the 2nd ring			Wavelength optimized for the 4th ring					
Ring #	Power density (W/mm ²)	Power (W)	Ring #	Power density (W/mm ²)	Power (W)			
1	0,00E+00	0,00E+00	1	0,00E+00	0,00E+00			
2	1,44E-02	3,23E-08	2	0,00E+00	0,00E+00			
3	0,00E+00	0,00E+00	3	9,51E-04	2,14E-09			
4	2,97E-03	6,69E-09	4	1,92E-02	4,33E-08			
5	0,00E+00	0,00E+00	5	0,00E+00	0,00E+00			

TABLE 4: POWER EXTRACTED FROM THE FOCUSING GRATINGS USING A NANO-IMPRINTED LENSED-FIBER

Using the lensed-fiber, the power density radiated by the gratings has been increased up to ten times which should be high enough to activate the opsins once the neural probes are inserted inside the brain. The the losses due to the coupling efficiency have decreased of 10 dB which allows to reach total losses on the order of 45 dB.

C) Possible improvements and next steps for the project

In order to allow neural probes to interface more neurons at the same time and to manipulate them using different means with a high efficiency, further improvements are required.

1) How to obtain a better fiber-waveguide coupling efficiency?

A solution which could be coupled with the nano-lensed fiber would be to have focusing gratings at the input of the waveguide, as it has been explained in the ways to couple the fiber and the waveguide. This idea was developed in an article [74] where this kind of gratings were used to couple infrared light in a 240 nm thick GaAs/AlOx waveguide. Because the wavelengths used for the optogenetics and the materials are different for the neural probes, simulations to find the right parameters of the gratings are required. Also, the fiber must be at a 90° angle with respect to the gratings. A coupling efficiency higher

than 50% has been achieved.

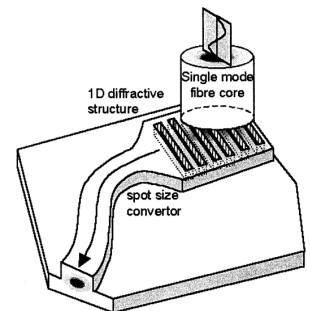


FIG.72: FOCUSING GRATING TO COUPLE LIGHT INSIDE THE WAVEGUIDE FROM THE OPTICAL FIBER [74]

2) Further modifications of the neural probes

In order to reach the multi-functionality of the neural probes required to manipulate the neurons and to sense the neural signals after these stimulations, developments must be done on the neural probes.

First, micro-fluidic channels to deliver drugs inside the brain must be integrated on the neural probes.

Also, multi-shank probes could allow to interface more neurons even though they imply more invasiveness when inserted inside the cortex of the brain. Some of them have been fabricated and one example is shown **Fig.73**:

The central shank includes an optical circuit whose rings have been successfully tested.

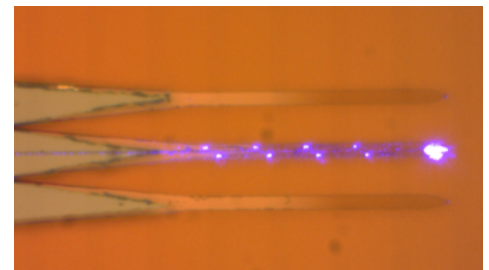


FIG.73: MULTI-SHANK OXIDE NEURAL PROBE WITH AN OPTICAL CIRCUIT ON THE CENTRAL SHANK

3) In-vivo tests of the optoelectronic probes

The very thin optoelectronic probes released (approximately 5 μm thick) have been inserted inside the mice brain to check if this thickness was an issue during the insertion of the probe inside the cortex of the brain: it was important to see if the probe would not break during the penetration of the dura mater. Out of three probes that have been tested, two could penetrate the dura without breaking; the third one first started to bend and then broke. This is a very promising result because having thinner probes should allow to reduce the inflammatory response of the brain after the probes are inserted inside the cortex. These results are summed up in the **Appendix 3**.

Electronic probes have already been tested on mice and neural signals have been successfully recorded. Now that optoelectronic probes have been released, it would be interesting to try these probes on genetically-modified mice to see if it is possible to activate some neurons with the focusing gratings in one specific area of the brain and then use the electrodes to check if an action potential has been triggered following this stimulation.

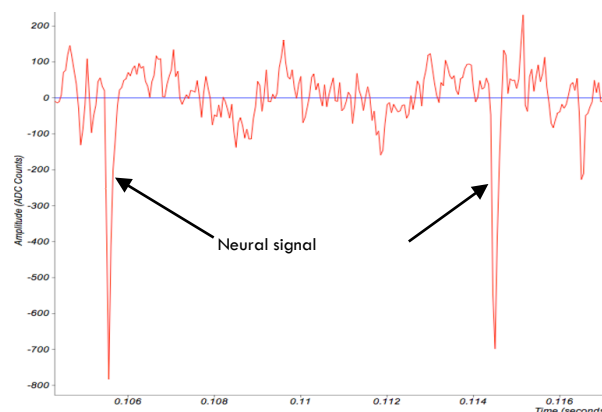


FIG.74: RECORDING OF NEURAL ACTIVITY INSIDE A MICE'S CORTEX USING ELECTRODES INTEGRATED ON A NEURAL PROBE [63]

V) CONCLUSION

During this internship, I have been involved in the fabrication of optoelectronic probes: these neural probes integrate optical components (waveguide, ring resonators and focusing gratings) to allow the manipulation of neurons inside some precise areas of the brain shining light on opsins and electrical components (electrodes) in order to sense the neural signals generated by the neurons' stimulation. These probes should allow us to understand better the functioning of the brain and, hopefully, to find therapies to cure diseases such as Parkinson's or epilepsy.

The probes that have been fabricated are very thin, and they should allow to reduce the inflammatory response of the body when they are inserted inside the cortex of the brain. Despite this thickness on the order of 5 μm , these probes have been successfully inserted inside the brain of mice without breaking, thanks to the help of a scientist from the *Department of Molecular and Cell Biology* from the Berkeley campus.

Etching a trench on the probes in order to connect an optical fiber to the waveguide allows to increase the stability of the fiber after gluing it: a high stability is required for this connection in order to be able to shine light inside the brain.

I have been involved in the tests of the optical components integrated on the probes have been tested: different ring resonators couple the light from the central waveguide of the shank of the probe depending on their diameter allowing to shine light inside different areas of the brain. The focusing gratings allow to focus light 20 μm far from the neural probe's shank to reach the neurons that have not been killed during the insertion of the neural probe inside the brain. The small diameter of the spot radiated by the focusing gratings should allow to reach a very small group of neurons to activate them. The power radiated by the focusing gratings when a nano-imprinted lensed-fiber is used to bring light inside the central waveguide of the shank is increased thanks to this technique and should be high enough to activate the opsins introduced inside the neurons; however, *in-vivo* tests must still be done to check this hypothesis.

Further steps include the integration of micro-fluidic channels on the shank of the neural probe to manipulate neurons at the synapse delivering drug in specific areas and the development of multi-shank neural probes in order to interface more neurons at the same time.

BIBLIOGRAPHY

- [1] <http://foundry.lbl.gov>
- [2] <https://ced.berkeley.edu/collaborate/collaboration-in-action/lbnl-second-campus>
- [3] Mohamed V, "The Edwin Smith Surgical Papyrus: Neuroscience in Ancient Egypt", in *IBRO History of Neuroscience*, June 2014
- [4] <http://connectomics.chalearn.org/help/tutorial>
- [5] Suzanaerculano-Houzel, "The Human Brain in Numbers: a Linearly Scaled-up Primate Brain", in *Human Neuroscience*, August 2009
- [6] <http://www.dreamstime.com/stock-illustration-glial-cells-brain-neurons-neuroglial-non-neural-there-different-types-oligodendrocyte>
- [7] <http://webpace.ship.edu/cgboer/theneuron.html>
- [8] *Bioelectronics and biomedical microelectronics*, class delivered by Professor Alexandre Schmid at the École Polytechnique Fédérale de Lausanne, 2017-2018
- [9] Drake K., Wise K., Farraye J., Anderson D., Bement S., "Performance of Planar Multisite Microprobes in Recording Extracellular Single-unit Intraortical Activity", in *IEEE Transactions on Bio-medical Engineering*
- [10] <https://en.wikipedia.org/wiki/Exocytosis>
- [11] Yan Chen, Lihong Liu, "Modern Methods for Delivery of Drugs Across the Blood-Brain Barrier", in *Advanced Drug Delivery Review*, May 2012
- [12] Zoltan Feteke, "Recent Advances in Silicon-Based Neural Microelectrodes and Microsystems: a Review", in *Elsevier*, March 2015
- [13] Georg Nagel, Doris Ollig, Markus Fuhrmann, Suneel Kateriya, Anna Maria Musti, Ernst Bamberg, Peter Hegemann, "Channelrhodopsin-1: A Light-Gated Proton Channel in Green Algae", in *Science*, June 2002
- [14] Video from Nature magazine video, "Method of the year 2010: Optogenetics", <https://www.youtube.com/watch?v=I64X7vHSHOE>
- [15] Peter Hegemann, Georg Nagel, "From Channelrhodopsins to Optogenetics", in the *US National Library of Medicine – National Institutes of Health*, January 2013
- [16] Song Luan, Ian Williams, Konstantin Nikolic, Timothy G. Constandinou, "Neuromodulation: Present and Emerging Methods", in *Frontiers in Neuroengineering*, July 2014
- [17] Eran Segev, Jacob Reimer, Laurent C. Moreaux, Trevor M. Fowler, Derrick Chi, Wesley D. Sacher, Maisie Lo, Karl Deisseroth, Andreas S. Tolias, Andrei Faraon, Michael L. Roukes, "Patterned Photostimulation via Visible-Wavelength Photonic Probes for Deep Brain Optogenetics", in *Neurophotonics*, 2016
- [18] https://www.photonics.com/Articles/Lasers_Optics_Enhance_Optogenetics_Studies/a57283
- [19] Linda Madisen, Tianyi Mao, Henner Koch, Jia-min Zhuo, Antal Berenyi, Yun-Wei Hsu, Algreto Garcia, Xuan Gu, Sebastien Zanella, Jolene Kidney, Hong Gu, Yimei Mao, Bryan Hooks, Edward Boyden, Jan Marino Ramirez, Allan Jones, Karel Svoboda, Xue Han, Eric Turner, Hungkui Zeng, "A Toolbox of Cre-Dependent Optogenetic Transgenic Mice for Light-Induced Activation and Silencing", in *Nature Neuroscience*, March 2012
- [20] https://en.wikipedia.org/wiki/Viral_vector
- [21] <https://en.wikipedia.org/wiki/Electroporation>
- [22] Yan Chen, Lihong Liu, "Modern Methods for Delivery of Drugs Across the Blood-Brain Barrier", in *Advanced Drug Delivery Review*, May 2012
- [23] Zoltan Feteke, "Recent Advances in Silicon-Based Neural Microelectrodes and Microsystems: a Review", in *Elsevier*, March 2015
- [24] <https://www.ncbi.nlm.nih.gov/pmc/articles/PMC5640165/>
- [25] Joshua Johansen, Hiroki Hamanaka, Marie Monfils, Rudy Behnia, Karl Deisseroth, Hugh Blair, Joseph LeDoux, "Optical Activation of Lateral Amygdala Pyramidal Cells Instructs Associative Fear Learning", in *Proceedings of the National Academy of Sciences of the United States of America*, May 2010
- [26] Warren Alilain, Xiang Li, Kevin P. Horn, Dhingra Rishi, Thomas E Dick, Stefan Herlitzte, Jerry Silver, "Light Induced Rescue of Breathing After Spinal Cord Injury", in *Journal of Neurosciences*, November 2012
- [27] Anish Thukral, Faheem Ershad, Nada Enan, "Soft Neural Interfaces for Ultrathin Electronics", in *IEEE Nanotechnology Magazine*, January 2018

- [28] Ahuva Weltman, James Yoo, Ellis Meng, "Flexible, Penetrating Brain Probes Enabled by Advances in Polymer Fabrication", in *Micromachines*, October 2016
- [29] <https://en.wikipedia.org/wiki/Electrocorticography>
- [30] https://en.wikipedia.org/wiki/Magnetic_resonance_imaging
- [31] https://en.wikipedia.org/wiki/Functional_magnetic_resonance_imaging
- [32] <http://www.brainybehavior.com/blog/2007/07/pet-scans-and-fmri-compared/>
- [33] <https://en.wikipedia.org/wiki/Magnetoencephalography>
- [34] <https://www.mayoclinic.org/diseases-conditions/temporal-lobe-seizure/diagnosis-treatment/>
- [35] <https://loupventures.com/bioelectronic-medicine-an-introduction/>
- [36] Dirk Saalfrank, Anil Krishna Konduri, Shahrzad Latifi, Rouhollah Habibey, Asiyeh Golabchi, Aurel Vasile Martiniuc, Alois Knoll, Sven Ingebrandt, Axel Blau, "Incubator-independent cell-culture perfusion platform for continuous long-term microelectrode array electrophysiology and time-lapse imaging", in *The Royal Society Open Science*, June 2015
- [37] <https://www.ncbi.nlm.nih.gov/books/NBK3901/>
- [38] Seongjun Park, Yuanyuan Guo, Xiaoting Jia, Han Kyoung Choe, Benjamin Grena, Jeewoo Kang, Jiyeon Park, Chi Lu, Andres Canales, Ritchie Chen, Yeong Shin Yim, Gloria B. Choi, Yoel Fink, Polina Anikeeva, "One-step Optogenetics with Multifunctional Flexible Polymer Fibers", in *Nature Neuroscience*, April 2017
- [39] <https://www.ncbi.nlm.nih.gov/pmc/articles/PMC3707475/>
- [40] Mohamad HajjHassan, Vamsy Chodavarapu, Sam Musallam, "NeuroMEMS: Neural Probe Microtechnologies", in *Sensors*, 2008
- [41] Micha Spira, Aviad Hai, "Multi-Electrode Array Technologies for Neuroscience and Cardiology", in *Nature Nanotechnology*, February 2013
- [42] Quan Qing, Sumon K. Pal, Bozhi Tian, Xiaojie Duan, Brian P. Timko, Tzahi Cohen-Karni, Venkatesh N. Murthy, and Charles M. Lieber, "Nanowire Transistor Arrays for Mapping Neural Circuits in Acute Brain Slices", in *Proceedings of the National Academy of Sciences of the United States of America*, December 2009
- [43] Christopher Chapman, Noah Goshi, and Erkin Seker, "Multi-functional Neural Interfaces for Closed-Loop Control of Neural Activity", in *Advanced Functional Materials*, August 2017
- [44] Firat Yazicioglu, Carolina Mora Lopez, Srinjoy Mitra, Bogdan Raducanu, Silke Musa, Fabian Kloosterman, "Ultra-High Density In-vivo Neural probes", in *IEEE Engineering in Medicine and Biology Society*
- [45] Saymour J., Kipke D., "Neural Probe Design for Reduced Tissue Encapsulation in CNS", in *Biomaterials*, September 2017
- [46] Ahuva Weltman, James Yoo, Ellis Meng, "Flexible, Penetrating Brain Probes Enabled by Advances in Polymer Microfabrication", in *Micromachines*, October 2016
- [47] Suzuki, T., Mabuchi, K., Takeuchi, S., "A 3D Flexible Parylene Probe Array for Multichannel Neural Recordings", in *Proceedings of the 1st International IEEE/EMBS Conference on Neural Engineering (NER)*, March 2003
- [48] Dion Khodagholy, Thomas Doublet, Pascale Quilichini, Moshe Gurfinkel, Pierre Leleux, Antoine Ghestem, Esma Ismailova, Thierry Herve, Sebastien Sanaur, Christophe Bernard, George Malliaras, "In-Vivo Recordings of Brain Activity Using Organic Transistors", in *Nature Communications*, March 2013
- [49] Mohamad HajjHassan, Vamsy Chodavarapu, Sam Musallam, "NeuroMEMS: Neural Probe Microtechnologies", in *Sensors*, 2008
- [50] James Jun, Nicholas Steinmetz, Joshua Siegle, Daniel Denman, Marius Bauza, Brian Barbarits, Albert Lee, Costas Anastassiou, Alexandru Andrei, Çağatay Aydın, Mladen Barbic, Timothy Blanche, Vincent Bonin, João Couto, Barundeb Dutta, Sergey Gratiy, Diego Gutnisky, Michael Häusser, Bill Karsh, Peter Ledochowitsch, Carolina Mora Lopez, Catalin Mitelut, Silke Musa, Michael Okun, Marius Pachitariu, Jan Putzeys, Dylan Rich, Cyrille Rossant, Wei-lung Sun, Karel Svoboda, Matteo Carandini, Kenneth Harris, Christof Koch, John O'Keefe, Timothy Harris, "Fully Integrated Silicon Probes for High-Density Recording of Neural Activity", in *Nature*, November 2017
- [51] Demetrios Papageorgiou, Susan Shore, Sanford Bledsoe, Kensall Wise, "A Shuttered Neural Probe with On-Chip Flowmeters for Chronic In-Vivo Drug Delivery", in *Journal of Microelectromechanical Systems*, August 2006
- [52] Lee Huynjoo, Son Yoojin, Kim Jeongyeon, Justin Lee, Yoon Eui-Sung, Cho Il-Joo, "A Multichannel Neural Probe with Embedded Microfluidic Channels for Simultaneous In Vivo Neural Recording and Drug Delivery", in *Lab on a Chip*, 2015

- [53] Bingzhao Li, Kwang Lee, Sotiris Masmanidis, Mo Li, "A Nanofabricated Optoelectronic Probe for Manipulating and Recording Neural Dynamics", in *Journal of Neural Engineering*, May 2018
- [54] John Seymour, Fan Wu, Kensall Wise, Euisik Yoon, "State-of-the-art MEMS and Microsystem Tools for Brain Research", in *Microsystems and Nanoengineering*, 2017
- [55] Robert Scharf, Tomomi Tsunematsu, Nial McAlinden, Martin Dawson, Shuzo Sakata, Keith Mathieson, "Depth-specific Control In-vivo with a Scalable, High-density μ LED Neural Probe", in *Scientific Report*, 2016
- [56] Fan Wu, Eran Start, Pei-Cheng Ku, Kensall Wise, Gyorgy Buzsa, Euisik Yoon, "Monolithically Integrated mLEDs on Silicon Neural Probes for High-Resolution Optogenetic Studies in Behaving Animals", in *Neuroresource*, December 2015
- [57] https://en.wikipedia.org/wiki/Cerebral_cortex
- [58] D.H. Szarowskia D.H., Andersena M.D., Retterer S., Spencec A.J., Isaacson M., "Brain responses to micro-machined silicon devices", in *Elsevier*, 2003
- [59] <https://photonics.lionix-international.com/mpw-service/>
- [60] Gray C.M., Maldonado P.E., Wilson M., McNaughton B., "Tetrodes Markedly Improve the Reliability and Yield of Multiple Single-Unit Isolation from Multi-unit Recordings in Cat Striate Cortex", in *Journal of Neuroscience Methods*, December 1995
- [61] Daldosso N., Melchiorri M., Riboli F., Sbrana F., Pavesi L., Pucker G., Kompocholis C., Crivellari M., Belluti P., Lui A., "Fabrication and Optical Characterization of Thin Two-dimensional Si_3N_4 Waveguides", in *Materials Sciences Semiconductor Process*, 2004
- [62] Paolo Micheletti's master thesis
- [63] Vittorino Lanzio's master thesis
- [64] <http://emlab.utep.edu/ee5390em21/Lecture%205%20--%20Coupled-mode%20theory.pdf>
- [65] David Lockwood, Lorenzo Pavesi, "Silicon Photonics II"
- [66] Vittorino Lanzio, "Optoelectronic Neural Probes with Passive Light Switching Optical Circuits: Light Control in Deep Brain Tissue", in *Journal of Micro/Nanolithography*, August 2018
- [67] Gyorgy Buzsaki, Eran Stark, Antal Berenyi, Dion Khodagholy, Daryl Kipke, Euisik Yoon, Kensal Wise, "Tools for Probing Local Circuits: High-Density Silicon Probes Combined with Optogenetics", in *Neuron*, April 2015
- [68] John Lyn, "A User's Guide to Channelrhodopsin Variants: Features, Limitations and Future Developments", in *Exp Physiology*, July 2010
- [69] <https://www.kth.se/mst/research/optics/apodized-waveguide-to-fiber-surface-grating-couplers-1.315473>
- [70] <https://www.frm.org/alzheimer/ampleur-maladie.html>
- [71] Saif I. Al-Juboori, Anna Dondzillo, Elizabeth A. Stubblefield, Gidon Felsen, Tim C. Lei, Achim Klug, "Light Scattering Properties Vary across Different Regions of the Adult Mouse Brain", in *Plos*, July 2013
- [72] [http://focenter.com/wp-content/uploads/documents/AngstromBond---Fiber-Optic-Center-Dymax-OP-4-20632-UV-Optical-Adhesive-\(3ml\)-Fiber-Optic-Center.pdf](http://focenter.com/wp-content/uploads/documents/AngstromBond---Fiber-Optic-Center-Dymax-OP-4-20632-UV-Optical-Adhesive-(3ml)-Fiber-Optic-Center.pdf)
- [73] Alexander Koshelev, Giuseppe Calafiore, Carlos Piña-Hernandez, Frances Allen, Scott Dhuey, Simone Sassolini, Edward Wong, Paul Lum, Keiko Munechika, Stefano Cabrini, "High-Refractive Index Fresnel Lens on a Fiber Fabricated by Nanoimprint Lithography for Immersvie Applications", in *Optics Letters*, Volume 41, Number 15
- [74] D. Taillaert, W. Bogaerts, P. Bienstman, T. F. Krauss, P. Van Daele, I. Moerman, S. Verstuyff, K. De Messel, R. Baets, "An Out-of-Plane Grating Coupler for Efficient Butt-Coupling between Compact Planar Waveguides and Single-Mode Fibers", in *Journal of Quantum Electronics*, July 2002
- [75] <https://www.corial.com/en/technologies/icp-rie-inductively-coupled-plasma-reactive-ion-etching/>
- [76] <http://www.oxford-instruments.cn/OxfordInstruments/media/plasma-technology/Process-news/Oxford-Instruments-Process-News-November-2011.pdf>

APPENDIX 1: TOOLS USED FOR THE PROJECT

Exposition tools

Tool 1: UV Photolithography

The explanations in this part have been taken from a class of *Optical Lithography* delivered by Professor Jumana BOUSSEY at the school Grenoble-INP Phelma.

The UV photolithography is a tool used to expose a resist (photon or electron sensitive material) to a certain pattern thanks to a UV source of light and through a mask. This is the preliminary step before etching in order to make sure the parts of the wafer that one does not want to etch will be protected. There are two kinds of photoresist:

- A photoresist is called “positive” if the part exposed to light get dissolved in the developer solution
- A photoresist is called “negative” if the part exposed to light does not get dissolved in the developer solution

The UV photolithography used is called “contact mode” because the mask used to pattern the photoresist is in contact with the wafer.

The advantages of this tool are:

- Simplicity
- High speed
- Affordable

The drawbacks of this tool are:

- Mask wear and contamination
- The resolution is limited by the mask resolution (hundreds of nm)

Tool 2: Electron-Beam Lithography

The electron-beam lithography is a tool used to expose a photoresist before etching. A beam of electron is focused on some parts of the resist and the resist is then developed.

With respect to the UV photolithography, the electron-beam lithography allows to have a much higher resolution, even below 10 nm. However, the throughput for this tool is very low which makes electron-beam lithography mainly used in a research environment.

Etching tools

Tool 1: Reactive Ion Etching (RIE)

The explanations in this part have been taken from a class of *Dry Etching* delivered by Professor Matteo Cocuzza at the school Politecnico di Torino.

Reactive Ion Etching, usually called RIE, is a dry etching technique which uses a plasma to etch the substrate instead of liquid chemicals. The plasma, consisting of a mix of different particles (electrons, neutral or ionized molecules, free radicals – highly reactive ...) is used in order to provide directionality to the etching: anisotropic etching can be done using the ions. In order to create a plasma, free electrons present in the chamber of the tool are accelerated thanks to the voltage applied between two electrodes; these electrons experience collisions with the other molecules in the chamber and create ions which are used to etch the layers of material.

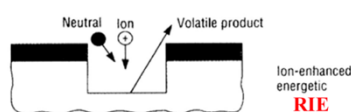


FIG.75: RIE PRINCIPLE

Tool 2: Inductively-Coupled Plasma Reactive Ion Etching (ICP RIE)

The ICP RIE is based on the same principle as the RIE: a plasma is created and the particles in the plasma are accelerated towards the substrate to etch it. The main difference for the ICP RIE with respect to the classic RIE is that a coil is used to create a magnetic field and increase the length of the path followed by the electrons to increase the number of collisions with the particles in the plasma and this way, more reactive species are created. In an ICP RIE, two different RF generators are used [75]:

- A 2 MHz generator applies power to the coil used to increase the path of electrons in the plasma and so allows to manage the ions fluxes
- A 13.56 MHz generator to extract ions from the plasma and accelerate them towards the substrate to etch the wafer

These two different RF generators allow to control independently the ion density and the ion energy allowing to reach higher etch rates, greater process flexibility and profile control, and reduced damage of the sample.

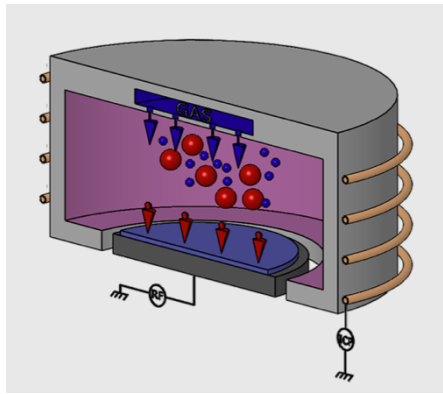


FIG.76: ICP RIE CHAMBER

Tool 3: Capacitively-Coupled Plasma (CCP RIE) or Viper

The CCP is similar to the ICP RIE because it allows to control separately the ions generation with a VHF power and the acceleration of the ions towards the substrate using a RF power: so the same functions are done just using a different technique: instead of using a coil, a VHF power is applied to the top electrode. At the *Molecular Foundry*, this tool is used to etch the dielectrics.

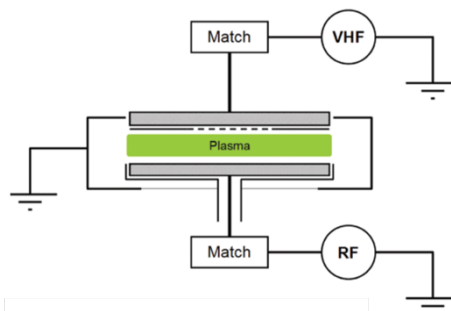


FIG.77: CCP USES VHF POWER TO BOOST PLASMA AND RF POWER TO CREATE A DC BIAS, LIKE AND ICP TOOL [76]

Deposition tools

Tool 1: Plasma-Enhanced Chemical Vapor Deposition (PECVD)

The PECVD is a technique using a plasma to obtain the species to be deposited on the substrate. This technique allows to have a high deposition rate at low temperature and to play with different parameters with respect to other techniques such as the Atomic Pressure Chemical Vapor Deposition or the Low Pressure Chemical Vapor Deposition; with the PECVD, the new parameters that can be controlled are the Radio Frequency power, the frequency and the bias. However, this is a complex tool to maintain and the quality of the film is not the best possible.

Tool 2: Evaporator

The explanations in this part have been taken from a class of *Epitaxy, Chemical Vapor Deposition and Electroplating* delivered by Professor Matteo Cocuzza at the school Politecnico di Torino.

The evaporator is a tool allowing to deposit thin films of metals on a substrate. The material to be deposited is held in a crucible: by properly selecting the current flowing in the crucible and so the temperature of the material, it is possible to evaporate it from the crucible and it is then deposited on the substrate. High deposition rates are reachable with this tool and several wafers can be exposed at the same time which allows a high throughput. However, not every material can be evaporated and a long time is required to obtain a high level of vacuum in the processing chamber (45 minutes at least).

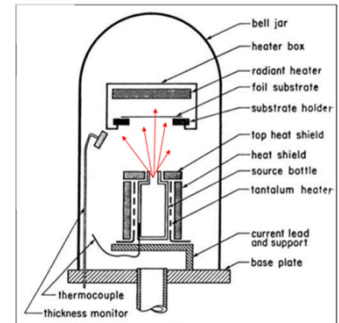


FIG.78: ELECTRON-BEAM EVAPORATOR PROCESS CHAMBER

Tool 3: Atomic Layer Deposition (ALD)

The explanations in this part have been taken from a class of *Materials for MEMS* delivered by Professor Fabrizio Giorgis at the school Politecnico di Torino.

In an ALD, gas pulses are delivered in a vacuum chamber in order to deposit one atomic layer of material at a time. A precursor is introduced into the process chamber and produces a monolayer on the wafer surface. A co-reactant is then introduced into the chamber reacting with the first precursor to produce a monolayer of film on the wafer surface.

There are two main mechanisms involved in the process:

- Chemisorption saturation process
- Sequential surface chemical reaction process

Since each pair of gas pulses (one cycle) produces exactly one monolayer of film, the thickness of the resulting film may be precisely controlled by the number of deposition cycles.

Characterization tools

Tool 1: Scanning Electron Microscope

The explanations in this part have been taken from a class of *Characterization of Technological Processes* delivered by Professor Fabrizio GIORGIS at the school Politecnico di Torino.

The SEM is a very powerful tool used to image the samples. With respect to optical characterization techniques, the SEM makes use of an electron-beam to analyse the samples: the scanning is non-destructive. The resolution reachable with the SEM makes it highly advantageous: indeed, the resolution is limited by the wavelength of the incident radiation and so the resolution of the SEM used at the *Molecular Foundry* is on the order of 20nm.

Tool 2: Profilometre

The profilometre is used to analyse the roughness of the surface of a sample. While the sample is held stable, a small tip in contact with the surface is moved along a certain axis and a sensor is used to keep track of the z-position of the tip allowing to determine the roughness of the surface.

APPENDIX 2: POWER COMPUTATION FROM THE GRATINGS

Once the alignment between the fiber and the waveguide is well done, i.e. the gratings can be seen using the CCD camera and the rings are switching (different spots are illuminating according to the laser's wavelength), pictures are taken at the different wavelengths. It is important to check that the gratings are not saturated, i.e. the when zooming on the spots, the colour of the pixels should not be higher than the maximum one (on a range from 0 to 255).

Using the software ImageJ, it is possible to split the colours of the pictures with the gratings in the three primary colors (blue, red, green). The interesting spots are the blue ones.

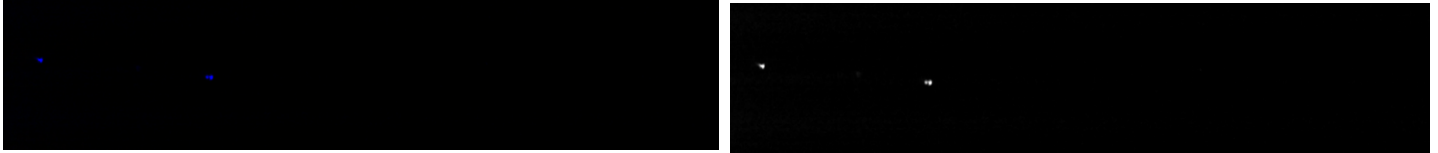


FIG.79: LEFT: ORIGINAL PICTURE SHOWING THE FOCUSING GRATINGS SHINING LIGHT. RIGHT: THE ORIGINAL PICTURE HAS BEEN MODIFIED SPLITTING THE CHANNELS

The first step is to calibrate the CCD camera used. To do so, the camera is focused on the optical fiber used: a spot is radiated out of the core of this fiber and a picture from this spot is taken.

Then, the average value of the pixel of the spot is measured using ImageJ as well as the area of the spot.

The power radiated by the fiber is computed with a powermetre and from the exposure time of the CCD camera, the energy radiated by the fiber is computed in Joule (Energy = Power x Exposure time). Then, from the energy, the average value of the pixels and the area of the spot, a conversion factor can be determined for any picture taken with the CCD camera from an integral.

For all the pictures of the spots, the average value of the pixel of the spot is measured as well as the area of the spot. Then, using the conversion factor computed previously, the power radiated by the spot is determined and from the estimated area of the spot in microns, $2\ \mu\text{m} \times 2\ \mu\text{m}$ (from the design of the focusing grating), the power density is computed in mW/mm^2 . This power density should be higher than $1.5\ \text{mW}/\text{mm}^2$ to activate the opsins.

APPENDIX 3: INSERTION OF THIN PROBES INSIDE A MICE'S BRAIN

In order to check if the thin probes – with a huge undercut etching the Silicon substrate - could be stiff enough to penetrate the dura, experimentation on mice have been done. The insertion was carried out by *Gregory Telian*, from the *Department of Molecular and Cell Biology* on the Berkeley campus.

To insert the probes inside the cortex of the brain, the scientist first needs to dig a hole in the skull. An anaesthesia is performed on the mice during the whole process of digging a hole. After the hole is done, one probe is inserted inside the brain using micromanipulators.

Unfortunately, after digging the hole, the mouse died so the probes' insertions have been performed on a dead one.

Overall, three trials have been done. The results are reported:

- 1st probe inserted: the probe penetrated the dura, no shank bending was observed during the insertion
- 2nd probe inserted: the probe bent to a 45° angle and did not penetrate the dura; another trial was performed using the same probe but the same issue occurred
- 3rd probe inserted: the probe penetrated the dura despite a small bending during the insertion.

According to *Gregory Telian*, the fact that two probes out of three penetrated so easily in the brain is even more impressive because the blood started to coagulate because of the mouse's death.

Using thinner probes allows to reduce the damages to the brain tissues and also to record more activity because multiple implantations can be done.

The insertion will be done again in the future following how the penetration damages the brain studying slices of it.

Master's thesis summary

To conclude my second year of *Master in Nanotechnologies for ICTs*, I did a six-month internship at the Nano-fabrication Facility of the Molecular Foundry, one of the lab composing the Lawrence Berkeley National Lab, in the city of Berkeley, in California, in the United States of America. The research topics in this laboratory focus on nano-structures and nano-materials: they go from the study of biological and inorganic nanostructures to the study of the nanostructured materials theory as well as the nano-fabrication and the nanostructures imaging.

The project I was involved in focused on the fabrication and on the characterization of neural probes, which are micro-systems implanted in the cortex of the brain in order to manipulate some neurons, for example by delivering drugs in some areas of the brain or by shining light on genetically-modified neurons to activate or to inhibit them and then, to measure the signals generated after these manipulations, mostly the action potentials triggered when the neurons communicate with each other.

First, a literature review has been done in order to understand the interests of such a project for the medical fields and for understanding how the brain is functioning. This literature review was also helpful to understand what were the different techniques to record the neural signals and why the neural probes were advantageous despite their huge invasiveness with respect to other techniques. Finally, I had to understand the many different fabrication steps required to release the optoelectronic neural probes.

Then, I have been working on the fabrication of these neural probes using the tools available in the cleanroom of the lab: deposition of SiO_2 layers using the Plasma-Enhanced Chemical Vapour Deposition, etching of the layers of SiO_2 and Si_3N_4 using respectively the CCP and the Reactive Ion Etching, etching of the Silicon layer using the Inductively-Coupling Plasma.

After the neural probes have been released, testing of the optical components embedded on them was required: it was necessary to check that the power density radiated out of the probes was high enough to activate or to inhibit genetically-modified neurons in mice's brain (the required power density is on the order of 1.50 mW/mm^2). To do so, I have used a tunable-wavelength laser connected to an optical fiber; this optical fiber was then approached in close proximity to the waveguide of the neural probes and I then tried to obtain the best alignment as possible between the two components to have a high coupling. The power density obtained with this probe's design being too low so a fiber nano-imprinted with a lens was used to have a better mode-matching between the fiber and the waveguide. This lens allowed to increase the power density radiated by ten and to reduce the coupling losses between the fiber and the waveguide.

After testing the optical components, the fiber must be glued to the waveguide for a later insertion in the cortex of the brain. With the first probes designed, the gluing was difficult due to a lack of mechanical contact between the fiber and the probe. This is why we have chosen to develop new design with a V-groove embedded on the probe to insert the fiber inside and increase the mechanical contact. This design has been developed using the software L-edit®.

After the new mask with the V-groove was available, new neural probes have been developed using the same recipes as for the previous wafer. However, after releasing the probes, we have noticed an important undercut and very thin probes have actually been fabricated which could be interesting to limit the invasiveness while performing the implantation of the probes in the brain: in the future, it could be interesting to try to insert these thin probes in the mice's brain to see if they do not break. The fiber gluing is easier with the new design.

This internship allowed me to progress in a very famous lab, close to researches highly-qualified in their field and with tools at the state-of-the-art. When I started this internship, my goal was to get more familiar with nano-fabrication tools and this is what happened: I feel more comfortable with the different processes and I understand better the advantages and drawbacks of certain tools with respect to others. During this internship, I also learned how to be more autonomous and scientifically more rigorous.

Résumé du stage

En conclusion de ma deuxième année de *Master en Nanotechnologies for ICTs*, j'ai effectué un stage de six mois à l'étage de Nano-fabrication de la Molecular Foundry, un des laboratoires faisant partie du Lawrence Berkeley National Lab, dans la ville de Berkeley, en Californie, aux États-Unis. Les sujets de recherche dans ce laboratoire sont focalisés sur les nano-technologies et nano-matériaux : ils vont de l'étude de nanostructures inorganiques et biologiques à l'étude de la théorie des matériaux nano-structurés, en passant par de la nano-fabrication et de l'imagerie de nanostructures.

Le projet sur lequel j'ai travaillé s'intéressait à la fabrication et à la caractérisation de sondes neuronales, qui sont des micro-systèmes implantés dans le cortex du cerveau pour manipuler certains neurones, par exemple en délivrant des médicaments dans le cerveau ou en illuminant des neurones génétiquement modifiés de manière à les activer ou les inhiber, et à mesurer les signaux électriques qui sont générés suites à ces manipulations, notamment les potentiels d'action qui sont déclenchés lorsque les neurones communiquent les uns avec les autres.

Dans un premier temps, il a fallu réaliser une recherche bibliographique afin de comprendre quels étaient les enjeux d'un tel projet pour la médecine et la recherche dans la compréhension du cerveau, quelles étaient aussi les différentes techniques pour lire les signaux qui sont générés dans le cerveau et quels étaient les intérêts des sondes neuronales en comparaison de ces autres techniques. Il a enfin fallu comprendre les différentes étapes qui étaient nécessaires à la fabrication de ces sondes.

Ensuite, j'ai travaillé sur la fabrication de ces sondes neuronales en réalisant différentes étapes sur les équipements disponibles dans la salle blanche du laboratoire : déposition de couches de SiO_2 avec le "Plasma-Enhanced Chemical Vapor Deposition", gravure des couches de SiO_2 et Si_3N_4 avec le "Capacitively-Coupled Plasma" et le "Reactive Ion Etching", gravure de la couche de Silicium avec le "Inductively-Coupling Plasma".

Après que les sondes aient été réalisées, il a fallu tester le fonctionnement des composants optiques et vérifier que ceux-ci permettaient de transmettre une densité de puissance assez importante pour pouvoir activer et/ou inhiber des neurones génétiquement modifiés (densité de puissance requise de 1.50 mW/mm^2). Pour cela, j'ai utilisé un laser - dont la longueur d'onde peut être changée - connecté à une fibre optique ; cette fibre optique a ensuite été approchée du guide d'onde présent sur les sondes neuronales et j'ai tenté d'obtenir le meilleur alignement possible entre ces deux entités afin de pouvoir voir des spots lumineux en sortie des "focusing gratings". La densité de puissance obtenue étant trop faible, des tests ont été réalisés avec une fibre sur laquelle a été nano-imprimée une lentille afin de faire correspondre le mode de la fibre et le mode du guide d'onde pour avoir un meilleur couplage entre la fibre et le guide d'onde. Cela a permis de réduire les pertes et d'augmenter la densité de puissance radiée par 10.

Après le test des composants optiques, il a fallu essayer de coller la fibre au guide d'onde : cette étape est nécessaire car après insertion dans le cerveau, la sonde est utilisée pour éclairer certaines zones particulières. Parce que le collage avec le premier design de sondes neuronales n'était pas assez stable, une sonde avec une fente pour permettre de glisser la fibre dedans a été développée. Ce design devait permettre d'augmenter le contact mécanique entre la fibre et la sonde et ainsi faciliter le collage. Ce nouveau design a été réalisé avec le logiciel L-edit®.

Une fois le nouveau masque réalisé, de nouvelles sondes ont été développées en appliquant les mêmes recettes que pour le précédent wafer. Cependant, un "undercut" important a été observé et des sondes très fines ont été développées, cela pourrait être un bon point pour limiter l'invasion au moment de l'implantation de ces sondes dans le cerveau : il faudra donc dans le futur explorer un peu plus loin ce résultat pour voir s'il est possible de le reproduire et si les sondes ne se cassent pas au moment de l'implantation dans le cerveau. Le collage de la fibre optique a été facilité avec ce nouveau design.

Ce stage m'a permis d'évoluer dans un laboratoire de renom, au contact de chercheurs reconnus dans leur domaine et avec des équipements à la pointe de la technologie. En commençant ce stage, mon but était de me familiariser avec des équipements de nano-fabrication et c'est ce qu'il s'est passé : je suis désormais plus à l'aise avec les différents processus et je comprends mieux les avantages de chaque équipement, notamment lorsqu'il s'agit de réaliser le "etching" des différentes couches de matériaux. Durant ce stage, j'ai aussi appris à faire preuve d'autonomie et de rigueur scientifique.

Tirocinio riassunto

Al fine di concludere il mio secondo anno di Master in Nanotecnologie, ho lavorato nell'ambito della nanofabbricazione alla Molecular Foundry, uno dei laboratori compresi nel complesso dei Laboratori Nazionali di Berkeley in California. Il soggetto della mia ricerca si è focalizzato su nanostrutture e nanomateriali spaziando dallo studio di strutture biologiche e inorganiche allo studio della teoria dei materiali nanostrutturati fino a nanofabbricazione e utilizzo di strumenti per la microscopia sulla nanoscala.

Il progetto in cui ho preso un ruolo attivo è stato focalizzato sulla fabbricazione e caratterizzazione di microsistemi che possono essere impiantati nella corteccia del cervello per poter stimolare e studiare la risposta neurale, ad esempio tramite trasporto di composti chimici in queste zone del cervello o illuminando dei neuroni geneticamente modificati al fine di attivarli o inibirli con lo scopo di poter misurare il segnale attivato da queste eccitazioni.

In una prima fase è stato essenziale uno studio di articoli di letteratura per poter capire l'interesse che c'è dietro tali progetti nel campo della medicina e per conoscere come funziona il nostro cervello. Questo studio di letteratura è stato utile per poter capire le differenti tecniche utilizzate per registrare i segnali neurali e per quale motivo queste sonde neurali possono essere vantaggiose nonostante siano invasive rispetto ad altre tecniche. In fine, ho dovuto comprendere le differenti tecniche e step di fabbricazioni necessari per poter rilasciare queste sonde neurali optoelettroniche.

In una seconda fase ho lavorato sulla fabbricazione di queste sonde usando diversi strumenti disponibili nella cleanroom del laboratorio: deposizione di SiO_2 utilizzando Plasma-Enhanced Chemical Vapour Deposition, etching di strati di SiO_2 e Si_3N_4 utilizzando rispettivamente CCP e Reactive Ion Etching, etching del silicio utilizzando Inductively-Coupling Plasma.

Una volta terminate la fase di fabbricazione è stato necessario caratterizzare otticamente il dispositivo tramite la misura della densità di potenza irradiata dalla componente ottica della sonda. Lo scopo di questa è vedere se la potenza in uscita è sufficiente per attivare o inibire i neuroni geneticamente modificati nel cervello dei topi (la densità di potenza richiesta è dell'ordine di $1.50\text{mW}/\text{mm}^2$). Al fine di fare ciò, ho utilizzato un laser a lunghezza d'onda variabile connesso ad una fibra ottica; questa fibra ottica è stata poi avvicinata alla guida d'onda nella sonda per poi ottenere l'allineamento tra le due. La densità di potenza ottenuta in questo modo non era sufficiente così è stato necessario usare una fibra diversa che potesse garantire un buon accoppiamento tra questa e guida d'onda. Questo tipo di fibra ha permesso l'aumento della densità di potenza irradiata di 10 volte riducendo così le perdite di accoppiamento fibra e guida d'onda.

Dopo una fase di test dei componenti ottici le fiber sono state incollate alla guida d'onda per poterle inserire nella corteccia del cervello. Inizialmente questa fase di incollaggio è stata difficile a causa di una mancanza di contatto meccanico tra fibra e sonda. Per questo abbiamo scelto di sviluppare un nuovo approccio con scavi a V nelle sonde per poter inserire le fiber all'interno e aumentare il contatto meccanico. Tale design è stato sviluppato utilizzando il software L-edit®.

In seguito alla realizzazione della nuova maschera per scavi a V sono stati realizzate nuove sonde neurali su un nuovo wafer. Tuttavia, dopo averle rilasciate, abbiamo notato un importante scavo eccessivo in fase di etching che ha portato a delle sonde estremamente sottili e che potrebbero avere degli interessanti riscontri in termini di bassa invasività durante l'impiantazione nel cervello: per il futuro sarà interessante vedere se è effettivamente possibile inserirle nel cervello dei topi senza che vi sia una rottura del dispositivo. Inoltre con questo nuovo design è possibile incollare più facilmente le fiber ottiche.

Questa esperienza mi ha permesso di contribuire all'interno di un laboratorio molto famoso, a stretto contatto con ricerca di alto livello e stato dell'arte di dispositivi per nanofabbricazione e nanocaratterizzazione. Quando ho iniziato il mio obiettivo era quello di imparare bene i dispositivi di nanofabbricazione e questo è esattamente ciò che è successo: ora conosco molti processi e riesco a comprendere vantaggi e svantaggi nell'utilizzo di diversi strumenti. Un'ulteriore cosa importante che ho imparato è il rigore scientifico e l'essere autonomo.

Gantt Diagram

